



**HAL**  
open science

## Reconstruction of the Provence Chain evolution, southeastern France

L. Bestani, N. Espurt, J. Lamarche, O Bellier, F. Hollender

► **To cite this version:**

L. Bestani, N. Espurt, J. Lamarche, O Bellier, F. Hollender. Reconstruction of the Provence Chain evolution, southeastern France. *Tectonics*, 2016, 35 (6), pp.1506-1525. 10.1002/2016TC004115 . hal-01792864v1

**HAL Id: hal-01792864**

**<https://hal.science/hal-01792864v1>**

Submitted on 15 May 2018 (v1), last revised 18 Jan 2019 (v2)

**HAL** is a multi-disciplinary open access archive for the deposit and dissemination of scientific research documents, whether they are published or not. The documents may come from teaching and research institutions in France or abroad, or from public or private research centers.

L'archive ouverte pluridisciplinaire **HAL**, est destinée au dépôt et à la diffusion de documents scientifiques de niveau recherche, publiés ou non, émanant des établissements d'enseignement et de recherche français ou étrangers, des laboratoires publics ou privés.

1 **Reconstruction of the Provence Chain evolution, southeastern France**

2

3 **L. Bestani<sup>1</sup>, N. Espurt<sup>1</sup>, J. Lamarche<sup>1</sup>, O. Bellier<sup>1</sup>, and F. Hollender<sup>2,3</sup>**

4

5 <sup>1</sup>Aix-Marseille Université, CNRS, IRD, CEREGE UM34, 13545 Aix en Provence, France

6 <sup>2</sup>Commissariat à l'Énergie Atomique et aux Énergies Alternatives (CEA), 13108 Saint Paul

7 lez Durance Cedex, France.

8 <sup>3</sup>Univ. Grenoble Alpes, ISTerre, CNRS, IRD, IFSTTAR. 38000 Grenoble, France.

9

10 Corresponding author: Nicolas Espurt (espurt@cerege.fr)

11

12

13 **Key Points:**

- 14 • First lithospheric-scale balanced cross-section of the Provence Chain
- 15 • Paleozoic structural control of subsequent episodes of deformation
- 16 • Orogenic crustal shortening of 155 km from the Late Cretaceous to Eocene

17

18 **Abstract**

19

20 The Provence fold-and-thrust belt forms the eastern limit of the Pyrenean orogenic system in  
21 southeastern France. This belt developed during the Late Cretaceous–Eocene Pyrenean–  
22 Provence compression and was then deformed by Oligocene–Miocene Ligurian rifting events  
23 and Neogene to present-day Alpine compression. In this study, surface structural data, seismic  
24 profiles, and crustal-to-lithospheric-scale sequentially balanced cross-sections contribute to  
25 the understanding of the dynamics of the Provence Chain and its long-term history of  
26 deformation. Balanced cross-sections show that the thrust system is characterized by various  
27 structural styles, including deep-seated basement faults that affect the entire crust, tectonic  
28 inversions of Paleozoic–Mesozoic basins, shallower décollements within the sedimentary  
29 cover, accommodation zones, and salt tectonics. This study shows the prime control of the  
30 structural inheritance over a long period of time on the tectonic evolution of a geological  
31 system. This includes mechanical heterogeneities, such as Variscan shear zones, reactivated  
32 during Middle Cretaceous Pyrenean rifting between Eurasia and Sardinia. In domains where  
33 Mesozoic rifting is well marked, inherited basement normal faults and the thermally weak  
34 crust favored the formation of an inner thick-skinned thrust belt during Late Cretaceous–  
35 Eocene contraction. Here, 155 km (~35%) of shortening was accommodated by inversion of  
36 N-verging crustal faults, N-directed subduction of the Sardinia mantle lithosphere and ductile  
37 thickening of the Provence mantle lithosphere. During the Oligocene, these domains were still  
38 predisposed for the localized faulting of the Ligurian basin rifting and the seafloor spreading.

39

40 **1. Introduction**

41

42 The fold-and-thrust belt preserved in the Provence basin forms the eastern limit of the  
43 Pyrenean orogenic system in southeastern France, between the Alps to the northeast and the  
44 Ligurian basin passive margin to the south (Fig. 1) [Mattauer and Proust, 1967; Séguret,  
45 1972]. The principal phase of shortening in the Provence segment occurred during the  
46 Campanian–Eocene period (named the Pyrenean–Provence compression), and this has been  
47 attributed to the collision between the Sardinia–Corsica continental block and Eurasia, and  
48 NW-directed subduction of the Tethys (at least south of the Sardinia) (Fig. 2) [Lacombe and  
49 Jolivet, 2005; Schettino and Turco, 2011; Schreiber et al., 2011; Molli and Malavieille, 2011;  
50 Advokaat et al., 2014]. This subduction system was connected eastward with the E-directed  
51 Alpine subduction [Lacombe and Jolivet, 2005]. In contrast to the western Pyrenean segment,  
52 which underwent shortening until Miocene times as a result of the collision between Eurasia  
53 and Iberia [Deselgaux et al., 1989; Muñoz, 1992], the eastern Provence segment was affected  
54 by the opening of the N-trending West European rift, and then by the NE-trending back-arc  
55 rifting of the Ligurian basin and the seafloor spreading that was associated with the counter-  
56 clockwise rotation of the Sardinia–Corsica block during the Oligocene–Miocene period  
57 [Hippolyte et al., 1993; Gattacceca et al., 2007]. This last major rifting event prevents any  
58 direct structural continuity between the Pyrenees and Provence belts. As a result, the inner  
59 structures of the Provence belt are now found in the Ligurian offshore basin and Sardinia–  
60 Corsica where some Pyrenean–Provence thrusts are suspected (Fig. 2) [Lacombe and Jolivet,  
61 2005]. The Eurasia–Adria collision and growth of the Alps were responsible for renewed  
62 Neogene to present-day shortening and deformation mainly in western Provence [Bergerat,  
63 1987; Champion et al., 2000] and in localized salt basins in eastern Provence [Angelier and  
64 Aubouin, 1976]. The superimposition of these later tectonic phases strongly modified the

65 overall geometry of the Provence Chain and makes it difficult to unravel its complete  
66 geological history.

67 The Provence Chain is a hybrid thick-skinned and thin-skinned belt [*Bestani et al.*,  
68 2015]. This structural setting was influenced by the pre-existing basin architecture, which  
69 included reactivation of the Late Paleozoic crustal faults and heterogeneous Mesozoic  
70 sedimentary pile [*Tempier*, 1987; *Roure and Colletta*, 1996].

71 Exhumation history of the sedimentary and basement units in Provence, Corsica and  
72 Sardinia is well constrain by low-temperature thermochronometry data including zircon and  
73 apatite fission track and apatite (U–Th)/He data [*Lucazeau and Mailhé*, 1986; *Morillon*, 1997;  
74 *Jakni*, 2000; *Zarki-Jakni et al.*, 2004; *Fellin et al.*, 2005; *Danišik et al.*, 2007; *Bestani*, 2015;  
75 *Malusà et al.*, 2016]. Three groups of cooling ages can be distinguished: old ages ranging  
76 between 110 and 244 Ma, intermediate ages ranging between 35 and 80 Ma, and young ages  
77 ranging between 10 and 30 Ma. Old ages are found in Mesozoic cover and in Paleozoic  
78 basement of eastern Provence and Sardinia. These ages are interpreted as detrital ages in the  
79 cover units or as long-term erosion episodes in the basement units prior Late Cretaceous  
80 followed by small reburial below the Mesozoic–Cenozoic sedimentary cover [*Danišik et al.*,  
81 2007; *Bestani*, 2015; *Malusà et al.*, 2016]. Intermediate ages are found in Paleozoic basement  
82 units of Provence, Corsica and Sardinia. They are related to the Late Cretaceous–Eocene  
83 structural growth and erosion of the Pyrenean–Provence wedge also recorded by distributed  
84 growth-strata deposits in Provence and Sardinia [*Espurt et al.*, 2012 and references therein;  
85 *Bestani*, 2015; *Malusà et al.*, 2016]. Oligocene–Neogene cooling ages are found along the  
86 southeastern Provence coast and in Corsica and Sardinia. These young thermochronometric  
87 ages are related to a reheating and/or erosion episode during the back-arc rifting of the  
88 Ligurian basin associated with major volcanism [*Jakni*, 2000; *Zarki-Jakni et al.*, 2004;  
89 *Malusà et al.*, 2016].

90           Apart from regional structural geometry descriptions and some balancing and  
91 restoration tests [e.g., *Tempier, 1987; Roure and Colleta, 1996; Lacombe and Jolivet, 2005;*  
92 *Terrier et al., 2008; Molliex et al., 2011; Espurt et al., 2012; Bestani et al., 2015*], a  
93 comprehensive study of the structure, quantification of the shortening, and definition of the  
94 role of crustal-lithospheric inheritances in this outstanding segment of the Pyrenean orogenic  
95 system have not been achieved yet.

96           The aim of this paper is to reconstruct the crustal-scale to lithospheric-scale structural  
97 architecture, the kinematics, and the shortening of the Provence Chain, using surface,  
98 subsurface and deep geophysical data, and balanced cross-sections together with  
99 paleogeographic reconstruction maps. This study has allowed us to evaluate the role of pre-  
100 existing rift basin architecture on the evolution of this polyphase segment of the Pyrenean  
101 thrust belt, and it provides an insight into the Pyrenean and Mediterranean geodynamics along  
102 the Eurasian–Sardinian plate boundary.

103

## 104 **2. Geological setting**

105

### 106 **2.1. Regional background**

107 The Provence basin can be separated into two structural domains according to the NE-  
108 trending Middle Durance and Aix-en-Provence faults, which is a major fault system that  
109 overlies a Paleozoic basement grain [*Arthaud and Matte, 1975; Guignard et al., 2005;*  
110 *Cushing et al., 2008; Terrier et al., 2008; Guyonnet-Benaize, 2011*] (Fig. 1). These two  
111 domains can be defined as follows:

112       - The southeastern domain corresponds to a complex tectonic domain made up of a thin  
113 (<4 km thick) Mesozoic to Cenozoic sedimentary cover and Variscan Maures and Tanneron-  
114 Esterel massifs to the southeast [*Roure et al., 1992; Masclé and Vially, 1999*]. It is bounded

115 by the Alps to the north-northeast (Fig. 1). This domain is composed of an array of  
116 multidirectional structures that are oriented from N010°E to N120°E. The deformation of the  
117 cover was mainly defined by deep-seated basement thrusts that were associated with cover  
118 décollements and salt tectonics [*Angelier and Aubouin, 1976; Tempier, 1987; Jannin, 2011;*  
119 *Espurt et al., 2012; Bestani et al., 2015*]. From south to north, the southeastern thick-skinned  
120 belt consists of a series of basin structures: Cap Sicié (western edge of the Hercynian Maures  
121 massif), Beausset basin, Sainte–Baume, Aurélien Mount, Etoile, Nerthe, Arc basin, Sainte–  
122 Victoire, Concors, Mirabeau–Vautubières, Vinon, Gréoux, and Valensole (Fig. 1). This  
123 domain shows structural and stratigraphic similarities with the Sardinia [*Lacombe and Jolivet,*  
124 *2005; Carosi et al., 2005; Malusà et al., 2016*].

125 - The northwestern domain corresponds to a trapezoidal panel made of a thicker (>7 km  
126 thick) Mesozoic-Cenozoic sedimentary cover that is bounded by the Baronnies basin to the  
127 north and the Nîmes fault to the west [*Masclé and Vially, 1999*] (Fig. 1). The sedimentary  
128 cover is deformed by E-trending spaced, long-wavelength thrust-related anticlines and salt  
129 tectonic structures [*Tempier, 1987; Rangin et al., 2010*]. From south to north, this domain  
130 comprises: Istres basin, Fare, Costes, Trévaresse, Luberon, Apt basin, Vaucluse Mountains,  
131 Carpentras basin, and Ventoux–Lure range structures (Fig.1).

132

## 133 **2.2. Lithostratigraphy and geodynamics of the Provence basin and Sardinia**

134 In the Provence basin, the oldest rocks are the Variscan granite and metamorphic series that  
135 are exposed in the southeastern Tanneron, Maures and Cap Sicié massifs, close to the present-  
136 day coastline (Fig. 1) [*Onézime et al., 1999; Rolland et al., 2009*]. These are unconformably  
137 overlain by ~1-km-thick Late Carboniferous to Permian volcanoclastic and detrital series and  
138 lower Triassic detrital series that were deposited in NNE-trending and ESE-trending graben

139 systems during the rifting phase of the Gondwana [*Delfaud et al.*, 1989; *Toutin-Mourin et al.*,  
140 1993; *Rolland et al.*, 2009; *Espurt et al.*, 2012; *Bestani et al.*, 2015].

141 The Mesozoic–Cenozoic lithostratigraphy of units that are exposed in the Provence  
142 basin is illustrated in logs of Figure 1. Middle Triassic–Early Cretaceous rocks were deposited  
143 during the opening of the Tethys ocean, Pyrenean rift to the west, and Valais domain to the  
144 northern Alps [*Handy et al.*, 2010; *Beltrando et al.*, 2012; *Bellahsen et al.*, 2014]. Triassic  
145 rocks are dominated by basal detrital series and upper evaporitic series, with Keuper facies  
146 mostly made up of gypsum and clays [*Arnaud et al.*, 1990]. This upper mechanically weak  
147 level was locally involved in surficial salt tectonic structures, like Suzette or Propiac diapirs  
148 [*Casagrande et al.*, 1989] (Fig. 1). The Jurassic and Early Cretaceous rocks consist of marine  
149 limestone in the eastern Provence, which evolves into thick basinal shale west of the Middle  
150 Durance fault system and toward the Vocontian basin, north of the Ventoux–Lure range (Fig.  
151 1) [*de Graciansky and Lemoine*, 1988; *Léonide et al.*, 2012]. North of the Ventoux–Lure  
152 range, and south of the Beausset syncline, locally the basin shows up to 1-km-thick Late  
153 Aptian–Albian turbiditic and basinal series, which include olistoliths and breccias [*Montenat*  
154 *et al.*, 1986; *Philip et al.*, 1987; *Montenat et al.*, 2004]. These series were deposited in graben  
155 systems [*Chorowicz and Mekarnia*, 1992; *Homberg et al.*, 2013] during the Middle  
156 Cretaceous rifting, as the Pyrenean rift system [*Debroas*, 1990; *Clerc et al.*, 2012].

157 Bauxite development marked the long-lasting stratigraphic hiatus, from at least the end  
158 of the Early Cretaceous to the beginning of the Late Cretaceous, which was related to the  
159 ‘Durance uplift’ between the Vocontian basin to the north and the Pyrenean rift system to the  
160 south [*Masse and Philip*, 1976; *Chorowicz and Mekarnia*, 1992; *Guyonnet-Benaize et al.*,  
161 2010]. The bauxite is covered by Middle Cenomanian–Santonian transgressive marine  
162 sediments that range from a maximum of ~1.1 km in thickness in the Beausset syncline (Fig.  
163 1), which progressively onlapped northward [*Philip*, 1970; *Floquet et al.*, 2005]. Locally, the

164 southern limb of the Beausset syncline comprises massive Turonian–Coniacian  
165 conglomerates (La Ciotat conglomerates) and Santonian sands (Fig. 1). These terrigenous  
166 deposits record the erosion of a southward emerged basement high between Provence and the  
167 Sardinia [Hennuy, 2003].

168 Foreland deposition started in the uppermost Santonian in a marine environment, and  
169 evolved into a general continental environment from the Campanian to Eocene, during  
170 northward propagation of the Pyrenean–Provence deformation front [Bestani *et al.*, 2015].  
171 The Campanian–Paleocene series display massive alluvial fans with growth stratal geometries  
172 close to thrust-related anticlines, like the Etoile–Nerthe, Luberon, Sainte–Baume or Sainte–  
173 Victoire structures [Corroy and Philip, 1964; Clauzon and Gouvernet, 1973; Leleu *et al.*,  
174 2009; Espurt *et al.*, 2012] (Fig. 1).

175 The Oligocene times were characterized by thick fluvial conglomerates, shale,  
176 evaporite, and lacustrine limestone [Hippolyte *et al.*, 1993] that were deposited in an  
177 extensional basin during the West European rift, which then saw the back-arc rifting of the  
178 Ligurian basin between Provence and Sardinia–Corsica block (Fig. 2). The Miocene  
179 transgression was associated with a major planar erosional surface that was well developed in  
180 western Provence and was overlain by marine limestone and grainstone (Fig. 1) [Besson,  
181 2005, Oudet *et al.*, 2010; Demory *et al.*, 2011]. The Neogene compression related to the  
182 growth of the Alps, and it is locally recorded by the Neogene continental growth strata  
183 [Clauzon *et al.*, 2011]. A drastic sea-level fall related to the Messinian salinity crisis was  
184 responsible for the deep incised valleys in the present morphology of Provence [Clauzon *et*  
185 *al.*, 1996].

186 The Sardinia continental block is largely constituted by Variscan basement rock  
187 similar to the Maures massif [Carosi *et al.*, 2005; Rolland *et al.*, 2009; Rossi *et al.*, 2009]. The  
188 basement is overlain by thin Mesozoic platform sequences and Paleocene–Eocene syntectonic

189 series that show similarities with Provence [*Philip and Allemann, 1982; Busulini et al., 1984;*  
190 *Mameli et al., 2007*], and widespread Late Eocene to Quaternary volcano-clastic-series-filling  
191 grabens [*Cherchi et al., 2008*].

192

### 193 **2.3. Décollement levels**

194 Deep-seated basement faults inherited from the Late Carboniferous to Permian and the Early  
195 Triassic might have been preferentially reactivated during subsequent episodes of deformation  
196 [*Lacombe and Mouthereau, 2002*]. Upper Triassic series formed the main décollement level  
197 for thrusting during Pyrenean–Provence and Alpine compressions [*Tempier, 1987*].

198 Disharmonic shallower décollement levels are also found in the Middle Jurassic black shales  
199 and Berriasian limestones [*Espurt et al., 2012; Guyonnet-Benaize et al., 2015*].

200

## 201 **3. Datasets and methodology**

202

203 To constrain the structure of the Provence Chain, we used new field data, 1:50 000 Bureau de  
204 Recherches Géologiques et Minières geological maps, and exploration wells. We also used  
205 depth-converted seismic reflection profiles provided by the Commissariat à l'Énergie  
206 Atomique et aux Énergies Alternatives [*Guyonnet-Benaize et al., 2015*] (Fig. 1). The depth  
207 geometry was constrained using published geophysical data for the Moho discontinuity depth,  
208 as determined by gravity data and P-wave seismic tomography [*Tesauro et al., 2008;*  
209 *Garibaldi et al., 2010*], and for the crust-lithosphere thickness [*Jiménez-Munt et al., 2003*].

210 A balanced cross-section technique is used to restore the basin geometry to the initial  
211 stages and to estimate the horizontal movement (shortening and extension). All of the above-  
212 mentioned data were integrated to balance and restore two cross-sections across the external  
213 Provence fold-and-thrust belt (T1 and T2; ~120 km long) and a lithospheric-scale section

214 (T1'; ~400 km long) that included the Ligurian basin, and the Sardinia and Tethyan  
215 subduction systems (Figs. 1, 2a). For the Provence belt, we used new structural data and the  
216 previously published *Bestani et al.* [2015] section. For the Ligurian basin, the Sardinia  
217 domain, and the Tethyan subduction system, we integrated data published by *Rollet et al.*  
218 [2002], *Dèzes et al.* [2004], *Lacombe and Jolivet* [2005], *Bache et al.* [2010], and *Malusà et*  
219 *al.* [2016] (Figs. 1, 2). We also integrated tectonic reconstruction maps of *Choukroune et al.*  
220 [1990], *Matte* [2001], *Guillot and Menot* [2009], *Molli and Malavieille* [2011] and *Advokaat*  
221 *et al.* [2014] for location of the Sardinia during Late Paleozoic to present-day.

222         Balancing and restoration were performed using the 'Move' structural modeling  
223 software (Midland Valley Inc.) based on thrust tectonic concepts [*Dahlstrom*, 1969; *Boyer*  
224 *and Elliot*, 1982; *Suppe*, 1983; *Suppe and Medwedeff*, 1990; *Shaw et al.*, 2005], and bed-  
225 length and thickness conservation, and flexural slip algorithm for cover. Area-balance  
226 approach is used for the deep crust and mantle [*Butler*, 2013]. Cross-sections were  
227 sequentially restored using regional stratigraphic data (see below). To calculate total  
228 extension and shortening amounts, cross-sections T1 and T2 are pinned in Baronnies in the  
229 north and near the Mediterranean coast to the south; lithospheric-scale cross section T1' is  
230 pinned in Baronnies in the north and on southern edge of the Sardinia crust.

231         The section orientation is orthogonal to the fold axes, in order to be parallel to the Late  
232 Cretaceous–Eocene N-S tectonic transport direction [*Lacombe et al.*, 1992]. The Provence  
233 basin is characterized by major NNE-trending fault systems (Fig. 1). These faults controlled  
234 deposition of the Mesozoic series and Oligocene-Miocene series and thrusting during  
235 Pyrenean and Alpine compressions [*Lacombe and Jolivet*, 2005]. Although the kinematic of  
236 these oblique faults is clearly established, the quantification of the oblique movement is still  
237 not constrained. The Late Cretaceous–Eocene N-S shortening was mainly accommodated by  
238 regional NNE-trending left-lateral strike-slip faults in the boundary between Languedoc and

239 Provence (Cévennes and Nîmes faults) and in the eastern edge of Corsica (Fig. 2b) [*Lacombe*  
240 *and Jolivet, 2005*]. We assume that the oblique motion along the NNE-trending Middle  
241 Durance fault system is small at least west of the Valensole plateau [*Roure et al., 2012*] (Fig.  
242 1) and would not significantly affect the structural geometry but might affect the shortening  
243 estimates [*Wallace, 2008*].

244 Kinematic reconstruction of plate motion between Eurasia and Iberia-Corsica-Sardinia  
245 block indicates transcurrent motion at least during the Late Paleozoic [*Matte, 2001; Guillot*  
246 *and Menot, 2009*] and Late Jurassic, followed by orthogonal extensional stretching in the  
247 Middle-Late Cretaceous [*Jammes et al., 2009*]. Late Paleozoic and Late Jurassic periods  
248 which recorded major strike-slip motion, prevents precise reconstruction of the lithospheric-  
249 scale balanced cross-section before Early Cretaceous.

250

#### 251 **4. Structure and restoration of the Provence thrust system**

252

253 The following structural description of the Provence belt is separated into three parts from  
254 southeast to northwest, with regard to the geological map given in Figure 1 and the cross-  
255 sections in Figures 3 and 4: (1) the southeastern Provence domain, where the deformation is  
256 mainly controlled by deep thick-skinned thrusting; (2) the central Middle Durance fault  
257 system; and (3) the northwestern Provence domain, where the deformation is mainly thin-  
258 skinned.

259

##### 260 **4.1. The thick-skinned domain**

261 On the basis of the structural and stratigraphic data, the previously published balanced cross-  
262 section of *Bestani et al. [2015]* suggested that the structure of this domain is governed by  
263 deep-seated basement faults and salt structures (Figs. 1, 3). In the southern part of section T1

264 (Fig. 3), the Late Paleozoic normal faults controlling pre-Triassic sedimentary basin geometry  
265 beneath the Bandol, Sainte–Baume and Sainte–Victoire structures were deformed by gently  
266 S-dipping basement thrusts propagating with short-cut trajectories (Fig. 3). The Late  
267 Cretaceous–Eocene tectonic inversion of the inherited rift structures led to deep intercutaneous  
268 basement thrust wedges [Espurt *et al.*, 2012; Bestani *et al.*, 2015] and large thin-skinned  
269 thrust displacements through the complete transfer of the shortening from the basement faults  
270 to the cover décollements (i.e., the Bandol, Sainte–Baume, Aurélien Mount, and eastern  
271 Sainte–Victoire thrusts; Figs. 1, 3). Salt tectonic structures are found beneath the Bandol and  
272 Sainte-Baume thrusts [Bestani *et al.*, 2015].

273 In the southernmost part of section T2 (Fig. 4), the Nerthe structure shows structural  
274 and sedimentary affinities with the eastern thick-skinned domain [Tempier, 1987]. This  
275 structure corresponds to an E-trending anticline that is mainly constituted by Early to Middle  
276 Cretaceous series (Figs. 1, 4b, 5). Field data and cross-section construction suggest surficial  
277 southward thrusting in sedimentary cover on a  $\sim 5^\circ$  N-dipping ramp associated with small-  
278 scale N-vergent thrusts [Dufaure *et al.*, 1969; Guieu, 1973]. The Nerthe anticline lies above a  
279 basement structural high that is associated with thin Mesozoic series compared to the Istres  
280 basin located to the north [Tempier, 1987; Andreani *et al.*, 2010]. We propose that the Nerthe  
281 anticline is separated from the Istres basin by a major E-trending N-dipping Mesozoic normal  
282 fault (Figs. 4, 6). This normal fault controlled thickness variations of the Mesozoic series. As  
283 previously speculated by Tempier [1987], we propose that the Nerthe high and its pre-existing  
284 normal fault were decapitated by a later S-dipping basement thrust located at  $\sim 9.5$  km b.s.l.  
285 during the Pyrenean–Provence compression (Fig. 4). This thrust is assumed to have fed slip  
286 northward into the western Provence cover.

287 Salt tectonic structures related to Triassic series started to develop during the Jurassic  
288 to Late Cretaceous times, and were then reactivated during the Pyrenean–Provence

289 compression and Oligocene extension (e.g., Huveaune area; Figs. 1, 3) [*Jannin, 2011; Bestani*  
290 *et al., 2015*]. Pyrenean–Provence thrust activity is mainly recorded from Campanian to  
291 Eocene (Figs. 3b, 4b) by alluvial fan deposits that locally show spectacular growth strata  
292 patterns, as for the Sainte–Baume and Sainte–Victoire thrust-system areas [*Leleu et al., 2009;*  
293 *Espurt et al., 2012; Bestani et al., 2015*]. The Pyrenean–Provence thick-skinned structures  
294 were cut by extensional fault systems and grabens during the Oligocene (Fig. 5a, b), and then  
295 eroded (e.g., wave-cut platforms) and sealed by Aquitanian to Tortonian marine strata  
296 [*Besson, 2005; Oudet et al., 2010; Andreani et al., 2010*].

297

#### 298 **4.2. Aix-Middle Durance fault system**

299 The Aix-Middle Durance fault system (Fig. 1) has been studied on the basis of field, seismic-  
300 profile, and seismicity data [*Cushing et al., 2008; Rangin et al., 2010; Guyonnet-Benaize,*  
301 *2011*]. Southward, this fault system connects with the Nerthe–Etoile thrust system, as a  
302 ‘horse-tail’ system (Fig. 1). This fault system is interpreted as overlying a NE-trending Late  
303 Paleozoic basement grain like the Toulouse fault in the central Pyrenees [*Arthaud and Matte,*  
304 *1975; Burg et al., 1990*] (Fig. 2). It separates a thick sedimentary succession (>7 km thick) to  
305 the northwest, in contrast to the southeast (<4 km thick) [*Ménard, 1980; Le Pichon et al.,*  
306 *2010; Guyonnet-Benaize et al., 2015*], and forms the boundary between the thin-skinned and  
307 thick-skinned structural domains of Provence (Figs. 1, 3, 4).

308 Seismic profiles 71D10 and VL85J are located close to cross-section T1 (Figs. 1, 7),  
309 and these show that the Middle Durance fault zone is composed of a deep W-dipping  
310 basement fault and a shallow listric normal fault that branches within Triassic evaporites  
311 [*Roure et al., 1992; Benedicto et al., 1996; Roure and Colletta, 1996; Cushing et al., 2008;*  
312 *Guyonnet-Benaize et al., 2015*]. This basement fault was mostly active as a normal fault  
313 during Mesozoic times [*Roure et al., 1992*], which allowed deposition of a thick sedimentary

314 pile in the western Provence domain, whereas the sedimentary cover fault system was  
315 assumed to be reactivated during Oligocene and Miocene times [Guignard *et al.*, 2005;  
316 Cushing *et al.*, 2008]. The interpretation of seismic profile VL85J also suggests Late  
317 Paleozoic–Early Triassic extensional basins beneath the Middle Durance fault system (Fig. 7).  
318 These inferred basement structures do not show structural inversion [Rangin *et al.*, 2010;  
319 Guyonnet-Benaize *et al.*, 2015]. The Middle Durance fault zone domain is seismically active,  
320 as revealed by present-day small seismic events ( $M < 3.5$ ) distributed in the sedimentary  
321 cover, and the historic seismicity [Cushing *et al.*, 2008; Le Pichon *et al.*, 2010]. These data  
322 suggest structural decoupling between the crustal part and the cover part of this fault zone  
323 [Cushing *et al.*, 2008].

324

### 325 **4.3. The thin-skinned domain**

326 Northwest of the Aix-Middle Durance fault zone, the large-scale folding of the sedimentary  
327 cover is mainly controlled by the geometry of the underlying Triassic salt layer [Rangin *et al.*,  
328 2010]. The construction of balanced cross-sections together with sediment thickness data and  
329 subsurface data suggests that the basement–cover interface geometry of western Provence is  
330 poorly deformed [Tempier, 1987; Champion *et al.*, 2000; Terrier *et al.*, 2008; Rangin *et al.*,  
331 2010; Molliex *et al.*, 2011]. The basement–cover interface is located at ~6 km b.s.l. along  
332 section T1 (Fig. 3) and ~9 km b.s.l. along section T2 (Fig. 4), and at a depth of more than 10  
333 km b.s.l. under the southern edge of the Baronnies in the north.

334 The seismic profile 82SE4D in the southern part of section T2 (Fig. 6) indicates that  
335 the Istres basin is a large syncline that is composed of thick Mesozoic series [Terrier *et al.*,  
336 2008]. Its southern limb dips ~30° northward, while its northern limb dips 37° southward. The  
337 seismic profile highlights thickness variations in Middle to Late Jurassic series probably  
338 controlled at depth by a Triassic salt migration north of the Istres syncline. Northward, the

339 sedimentary cover is deformed by two ENE-trending and S-verging thrust-related anticlines  
340 (i.e., Fare and Costes anticlines) (Figs. 1, 4). The initial activation age of these structures is  
341 probably ante-Eocene as revealed by the discordance of the Miocene strata on deformed Early  
342 Cretaceous limestones [Dubois, 1966]. A small post-Miocene reactivation of the Costes  
343 anticline is attested by deformed Serravalian–Tortonian strata on its southern flank (Figs. 1, 4)  
344 [Dubois, 1966; Champion *et al.*, 2000].

345         The Luberon anticline forms a major curve-shaped range of about 65-km-long that is  
346 bounded by the Middle Durance fault zone to the east and the Salon–Cavaillon fault zone to  
347 the west (Fig. 1). Along cross-section T2, the western Luberon thrust is a broad S-verging  
348 breakthrough fault-propagation fold formed of thick lower Cretaceous limestone (Fig. 4). This  
349 anticline shows a 10° N-dipping backlimb and a 70° S-dipping forelimb. The forelimb shows  
350 locally massive (~300 m thick) Paleocene–Eocene breccia deposits with growth strata  
351 geometry that records the initial growth of the Luberon anticline during the Pyrenean–  
352 Provence compression [Clauzon and Gouvernet, 1973; Villegier and Andrieux, 1987]. The  
353 western Luberon anticline is globally covered by Burdigalian–Serravallian strata and Miocene  
354 wave-cut platforms [Besson, 2005]. Along section T1, the eastern Luberon structure is a N-  
355 verging thrust-related anticline associated with a S-verging back-thrust (Fig. 3). The recent  
356 compressional reactivation of eastern Luberon was recorded as before the Messinian salinity  
357 crisis [Clauzon *et al.*, 2011]. The 71D10 and VL85J seismic profiles reveal that the eastern  
358 Luberon ramp dips ~15° through the Middle Jurassic to Cenozoic series (Fig. 7). The thrust  
359 probably connects down in the Triassic evaporites along the Middle Durance fault zone.

360         The Apt basin is a 20-km-long and 40-km-wide slightly deformed syncline that is  
361 filled by ~600-m-thick Oligocene to Tortonian series (Figs. 1, 3). This basin was transported  
362 northward on the Ventoux–Lure thrust system, which is an E-trending 65-km-long range (Fig.  
363 1). The Ventoux–Lure range superimposes on a major Early Cretaceous paleogeographic limit

364 that delimited the Vocontian basin to the north (Baronnies) from the southern Provence  
365 Platform to the south [Arnaud, 1988; Ford and Stahel, 1995; Mascle and Vially, 1999]. Both  
366 cross-sections suggest that the overall geometry of the Ventoux–Lure hanging-wall consists  
367 of a  $\sim 5^\circ$  to  $10^\circ$  S-dipping homocline formed of massive Early Cretaceous marine limestone  
368 (Fig. 3). The Ventoux–Lure hanging-wall is deformed by the Vaucluse Mounts anticline to  
369 the west and by the NNE-trending Oligocene Sault graben in the center (Figs. 1, 4). The  
370 footwall of the Ventoux–Lure thrust corresponds to imbrications of closely spaced N-verging  
371 thrusts and narrow asymmetric synclines filled by Oligocene–Miocene series (Figs. 5c, 8).  
372 Preserved or tilted normal fault scarps are common between Mesozoic and Oligocene–  
373 Miocene series [Casagrande et al., 1989]. An Oligocene fault that cuts the Ventoux thrust  
374 shows major thrusting before the Oligocene; i.e., during the Pyrenean–Provence shortening  
375 (Figs. 5c, 8). In part, the reactivation of the Ventoux thrust is post-Miocene, as revealed by the  
376 deformed Miocene series [Villegier and Andrieux, 1987].

377         The geology of the southern edge of the Baronnies basin is characterized by E-  
378 trending fault-propagation folds and Jurassic–Early Cretaceous syn-sedimentary normal faults  
379 that were associated with salt migration, like the Propiac diapir in cross section T2  
380 [Casagrande et al., 1989] (Figs. 1, 4). Cross-section balancing suggests that the thick  
381 Mesozoic sedimentary infilling of the southern edge of the Baronnies zone was expelled  
382 southward without basement-fault reactivation, as suggested by Roure and Colletta [1996]  
383 and Mascle and Vially [1999]. Shortening was accommodated southward by internal thrust-  
384 folds, and in the Ventoux–Lure thrust as an intercutaneous wedge (Figs. 3, 4). Thrusting  
385 activity occurred during the Lutetian–Bartonian, as revealed by locally preserved syntectonic  
386 conglomerates with growth-strata patterns [Montenat et al., 2005] (Fig. 1), and during the  
387 Neogene [Villegier and Andrieux, 1987; Casagrande, 1989].

388

389 **4.4. Campanian-Eocene Pyrenean–Provence shortening versus Oligocene Ligurian and**  
390 **Neogene Alpine deformations**

391 The Provence fold-and-thrust belt recorded superimposed deformations from the Campanian  
392 to the present day, due to the Pyrenean–Provence and Alpine compressions, and to the rifting  
393 of the Ligurian basin. Cross-sections T1 and T2 of Figures 3 and 4 are restored just after and  
394 before the Campanian–Eocene compression, i.e., Late Eocene and latest Santonian,  
395 respectively. Assuming that the top of the uppermost Santonian series was horizontal before  
396 the shortening, restoration allows modeling of the pre-tectonic basement geometry before the  
397 Campanian–Eocene Pyrenean–Provence compression. The Late Eocene restorations allow the  
398 precise quantification of the Pyrenean–Provence shortening and the geometry of the Provence  
399 Chain before the Oligocene Ligurian and Neogene Alpine deformations.

400 The restoration of cross-sections T1 and T2 at the end of the Eocene indicates that the  
401 post-Eocene to present-day horizontal tectonic movement is small, at about 1.5 km (Figs. 3a,  
402 4b). The Oligocene extension is associated with high-dipping normal to strike-slip faults,  
403 delimiting grabens and half grabens, and local migration of Triassic salt [*Arnaud et al.*, 1990;  
404 *Bestani et al.*, 2015] (Fig. 5a,b). The Neogene Alpine deformation is minor, and is associated  
405 with reactivated inherited strike-slip faults, thrusts, and folding in the western thin-skinned  
406 Provence domain [e.g., *Champion et al.*, 2000; *Molliex et al.*, 2011] (Fig. 5c).

407 The total Pyrenean–Provence shortening ranges from 9.6 km (7.8%) in the west to  
408 46.4 km (26%) in the east (Figs. 3b, 4b, sections T1, T2, respectively). The western thin-  
409 skinned Provence domain shows a homogeneous along-strike shortening of about 6 km to 7  
410 km.

411

412 **4.5. Kinematics of the Provence thrust system**

413 The development and evolution of the fold-and-thrust belts might be significantly controlled  
414 by upper crustal inheritance that developed during the contractional stage or continental  
415 rifting and the geometry of the pre-orogenic sedimentary wedge [e.g., *Baby et al.*, 1989;  
416 *Coward*, 1996; *Colletta et al.*, 1997; *Ziegler et al.*, 1998; *Kley and Monaldi*, 2002; *Lacombe*  
417 *and Mouthereau*, 2002; *Butler et al.*, 2006; *Espurt et al.*, 2008]. The Provence foreland is  
418 characterized by contrasted Variscan and Mesozoic structural and sedimentary inheritances  
419 [*Roure and Colletta*, 1996; *Bestani et al.*, 2015]. Extensional basement faults inherited from  
420 Late Carboniferous–Permian to Early Triassic times controlled the location of the deformation  
421 during the Pyrenean–Provence compression and the synchronous activity of some thrusts over  
422 a long period of time (up to ~40 Myrs) [*Espurt et al.*, 2012].

423       Structural inheritance in Provence accounts for significant along-strike variations, in  
424 terms of the structural architecture, tectonic style, and shortening (Figs. 3, 4). The difference  
425 in tectonic style and shortening between sections T1 and T2 might be accommodated by left-  
426 lateral strike-slip motion along the NE-trending Aix-Middle Durance fault system south of the  
427 Valensole plateau (Fig. 1). Subsurface data and balanced cross-sections suggest that this fault  
428 system led to major thickness variations of the pre-orogenic Mesozoic pile between western  
429 and eastern Provence, due to the Mesozoic normal faulting (Figs. 1, 3, 4). No geological  
430 evidence that might support a Cenozoic reactivation of the deep Middle Durance basement  
431 fault is visible [*Roure and Colletta*, 1996]. This fault system had the role of an  
432 accommodation zone, *sensu Faulds and Varga* [1998], between the eastern thick-skinned  
433 domain and the western thin-skinned domain during the Pyrenean–Provence shortening. The  
434 footwall of the Aix-Middle Durance fault zone may have acted as a buttress to the N-S  
435 Pyrenean-Provence shortening [*Andreani et al.*, 2010], thus preventing the transfer of the  
436 thick-skinned shortening within the sedimentary cover of the western Provence. A small  
437 transfer of the thick-skinned shortening is only suspected in the Nerthe basement high

438 [Tempier, 1987]. The shortening difference of 40 km observed in cross-section T1 in  
439 comparison with cross-section T2 might be accommodated southward by thick-skinned  
440 basement thrusts that are now found in the offshore Ligurian basin and Sardinia [Tempier,  
441 1987; Lacombe and Jolivet, 2005].

442 This along-strike structural behavior is also illustrated by the present-day  
443 compressional tectonic regime in Provence. West of the Middle Durance fault zone, most of  
444 the deep-seated seismic events related to the Alpine shortening are located near the basement–  
445 sedimentary cover interface (~8 km deep), which emphasizes the basement–cover detachment  
446 [Terrier *et al.*, 2008; Cushing *et al.*, 2008; Molliex *et al.*, 2011]. East of the Middle Durance  
447 fault zone, the existence of seismic events below the Valensole plateau (Fig. 1) at a similar  
448 depth as to the west demonstrates present-day tectonic strain within the basement.

449

## 450 **5. Discussion: Reconstruction of the Provence Chain evolution**

451

452 Crustal structural inheritance can have major roles in the evolution of fold-and-thrust belts  
453 [Lacombe and Mouthereau, 2002; Butler *et al.*, 2006, and references therein; Espurt *et al.*,  
454 2014; Bellahsen *et al.*, 2014]. Little is known about the influence in terms of the geometry  
455 and thermal heterogeneities of the Provence crust and the associated Sardinia crust to the  
456 south [Garibaldi *et al.*, 2010; Le Pichon *et al.*, 2010]. To evaluate and discuss the control of  
457 the deep processes on the structure, building and evolution of the Provence Chain, we  
458 constructed a trans-orogenic (~400 km long) balanced cross-section T1' at the scale of the  
459 lithosphere along section T1, which included the geodynamic evolution of the Ligurian basin  
460 and Sardinia to the south (Fig. 9a).

461 In our construction, the geometry of the continental and oceanic crusts in the Ligurian  
462 basin under the post-Messinian series is modeled using lateral seismic reflection data of *Rollet*

463 *et al.* [2002] and *Bache et al.* [2010]. The geometry of Sardinia was simplified as a  
464 homogenous basement block that included the Mesozoic–Cenozoic sedimentary cover. On the  
465 basis of the above-mentioned deep geophysical data, along section T1 we calculated a present  
466 crustal area of  $\sim 3\,052\text{ km}^2$  for the Sardinia continental crust, and  $\sim 4\,513\text{ km}^2$  for the Eurasian  
467 continental crust (Fig. 9a).

468 The present-day geometry of the Eurasian continental crust is characterized by  
469 southward thinning, from  $\sim 35\text{ km}$  beneath the Baronnies basin to  $\sim 7\text{ km}$  beneath the north  
470 Ligurian basin passive margin (Fig. 9a) [*Jiménez-Munt et al.*, 2003; *Tesauro et al.*, 2008;  
471 *Garibaldi et al.*, 2010]. This crustal thinning might result from the Oligocene rifting and  
472 drifting of the Ligurian basin (by more than 200 km) that was associated with the counter-  
473 clockwise rotation of the Sardinia–Corsica block [*Rollet et al.*, 2002]. Similar thinning was  
474 observed west of the study area in the Gulf of Lion, by *Séranne et al.* [1995] and *Benedicto et*  
475 *al.* [1996] (Fig. 2a). In contrast to the Gulf of Lion, onshore the Pyrenean basement thrusts  
476 were less reactivated in Provence area. Oligocene structures might be hidden under thick post-  
477 Messinian sequences of the Ligurian basin [*Rollet et al.*, 2002].

478 Three stages of deformation of the Provence Chain can be reconstructed from the  
479 Triassic to the Eocene, which are illustrated in Figure 9 and discussed below. In this  
480 sequential restoration, we balanced the crustal areas of Eurasia and Sardinia through  
481 consecutive deformational episodes according to the paleo-thicknesses and erosion of the  
482 sedimentary cover and basement units along the margins of the Ligurian basin [e.g., *Jakni*,  
483 2000; *Bestani*, 2015; *Malusà et al.*, 2016].

484

485 *1. The Triassic stage* (post-Variscan structure): Late Paleozoic tectonic map reconstruction of  
486 Fig. 2d shows that the Eurasia–Provence and Sardinia crusts were separated by a major E- to  
487 NE-trending dextral shear zone [*Matte*, 2001; *Rossi et al.*, 2009; *Guillot and Menot*, 2009].

488 This major deformation zone is interpreted as the eastern continuation of the North-Pyrenean  
489 Fault Zone between Eurasia and Sardinia [*Lacombe and Jolivet, 2005*]. Tectonic map  
490 reconstruction indicates a dextral strike-slip component of more than 300 km. Because this  
491 shear zone prevents precise reconstruction of the lithospheric-scale balanced cross-section, we  
492 assume a simplified Triassic geometry for this deformation zone, which included surficial  
493 Late Carboniferous–Permian to Early Triassic half-grabens [*Bestani et al., 2015*] and a  
494 thinned crust, probably associated with ductile deformations (Fig. 9d).

495

496 *2. The Santonian stage* (Pyrenean rifting): According to Middle Cretaceous tectonic map  
497 reconstruction of Fig. 2c [*Advokaat et al., 2014*], the restoration before the Pyrenean–  
498 Provence compression shows a ~140 km-wide rift system with crustal hyperextension  
499 between Eurasia and Sardinia (Fig. 9c). This modeled rifting zone can be interpreted as the  
500 relay zone between the Pyrenean rift and Valais domain [*Stampfli et al., 1998; Rosenbaum et*  
501 *al., 2002; Bellahsen et al., 2014*], although the age of the Valais domain is debated (middle to  
502 late Jurassic or/and early Cretaceous) [e.g., *Beltrando et al., 2012* and references therein]. The  
503 Provence and Sardinia regions were uplifted and subject to major erosion associated with  
504 bauxites deposition since Albian and until the beginning of the Late Cretaceous (e.g.,  
505 ‘Durance uplift’). Our reconstruction is consistent with the paleogeography of *Hennuy* [2003],  
506 which included basement high located close to sea-level between the Provence and Sardinia.  
507 This massif constituted by Variscan rocks was eroded during the Middle Cretaceous–  
508 Santonian period, whence it fed terrigenous sediments at least into the Beausset basin in the  
509 north (Fig. 9c).

510 In this rifting context, the restoration suggests extreme crustal thinning of the southern  
511 Provence crust between the underlying mantle lithosphere and the Mesozoic sedimentary  
512 cover. In contrast to the Pyrenees, the Provence rift shows no field evidence for mantle

513 exhumation or ductile deformation at shallow crustal level [Duée *et al.*, 1984; Roure *et al.*,  
514 1989; Specht, 1989; Lagabrielle *et al.*, 2010; Clerc *et al.*, 2012; Vacherat *et al.*, 2014;  
515 Lagabrielle and Clerc, 2014] because these inner features have been erased by the Oligocene  
516 Ligurian rifting and drifting. On the basis of our cross-section restoration and  
517 paleogeographic reconstruction (Figs. 2, 9c), the N-S total crustal extension achieved in this  
518 zone between the Triassic and Santonian is estimated to be at least of 40-45 km. This  
519 partitioned rift model, including a central basement high between Provence and Sardinia, is  
520 similar to that proposed in eastern and central Pyrenees between the North-Pyrenean Fault to  
521 the south and Eurasia to the north [Clerc and Lagabrielle, 2014]. The extension amount  
522 calculated for Provence rift is close to the minimum values (~50 km) estimated in the eastern  
523 and central Pyrenees by Vergés and García-Senz [2001] and Mouthereau *et al.* [2014],  
524 respectively.

525

526 *3. The Eocene stage (post-Pyrenean–Provence compression):* From north to south, the Eocene  
527 restoration shows that the Provence orogen was formed by an outer thin-skinned thrust system  
528 that deformed a thick Mesozoic sedimentary cover north of the Aix-Middle Durance fault  
529 system, an inner N-verging thick-skinned system, and the Sardinia continental block bounded  
530 southward by the Tethys subduction system. As the Oligocene deformation in the outer  
531 Provence belt was small, the crustal geometry is similar to the present in this zone, although  
532 the inner basement thrust system thickened the crust to up to ~20 km (Fig. 9b).

533 During the inversion process, we propose a tectonic model where the previously  
534 extended and thermally weakened area was sandwiched between Eurasia and Sardinia. In this  
535 model, the strong Eurasia lithosphere [Le Pichon *et al.*, 2010] behaved as a lower tectonic  
536 wedge that indented the Sardinia continental block at the crust–mantle boundary [Roure *et al.*,  
537 2012]. We propose that the indentation of this lithospheric-scale tectonic wedge was

538 accommodated by inversion of N-verging crustal faults (e.g., Cap Sicié thrust), N-directed  
539 subduction of the dense Sardinia mantle lithosphere under the Provence and ductile  
540 thickening of the Provence mantle lithosphere (Fig. 9b). This model does not involve the  
541 mid-crustal detachment level as suggested previously by *Vially and Trémolières* [1996] across  
542 the entire Provence crust, but has crust/mantle interface detachment in the internal zone where  
543 the crustal thickness was reduced, and thrusts that cut through the crust of the Provence  
544 margin (Fig. 9b, c) [*Butler*, 2013]. The small crustal volume of Sardinia prevents the  
545 construction of an alternative balanced cross-section with underthrusting of crustal material of  
546 Sardinia beneath the Eurasian crust during the collision. However, the overthrusting of the  
547 Sardinia block on the Provence crust is consistent with apatite fission-track data along the  
548 western margin of Sardinia, which recorded the Late Cretaceous–Eocene cooling ages  
549 [*Malusà et al.*, 2016]. Our structural model in which the crust is decoupled from the mantle  
550 lithosphere during the Pyrenean–Provence orogeny is an efficient thickening mechanism that  
551 leads to the structural culmination of the inner thick-skinned Provence associated with a thin  
552 crust (Fig. 9b).

553         Although the structural model illustrated in Figure 9 includes neither precise geometry  
554 of the Middle Cretaceous hyperextended rift system at depth nor the internal structure of the  
555 Sardinia block, we calculate a N-S total crustal shortening in this sector of the Provence Chain  
556 of ~155 km (~35%) over the Late Cretaceous–Eocene period (Fig. 9b). This estimate of the  
557 Pyrenean–Provence contraction is a minimum value mainly because the original crustal  
558 thicknesses and rift geometry has to be better constrained. Most of this shortening is  
559 accommodated in the internal basement imbrication of the thick-skinned Provence belt.  
560 Ductile Triassic evaporites and thick sedimentary cover in western Provence might have  
561 favored the thin-skinned tectonic style and transfer of compressional stress in the Baronnies  
562 zone up to 100 km away from the inner orogenic wedge (Figs. 1, 9). In contrast to the

563 Pyrenees which involved the stacking of at least three S-verging crustal thrust sheets [e.g.,  
564 *Muñoz, 1992; Teixell et al., 2016*], the Provence Chain localized the overall crustal shortening  
565 along at least three N-verging thrust sheets (Fig. 9b). This northward structural stacking was  
566 controlled by inherited N-dipping weakness zones in Provence margin related to the Late  
567 Paleozoic and Mesozoic rifting events and the high rigidity of the Variscan basement of  
568 Sardinia [*Tesauro et al., 2009; Rossi et al., 2009*]. However, these structures might have been  
569 removed by erosion or Neogene deformation.

570         The minimum crustal shortening amount (~155 km) across the Provence Chain is  
571 higher than the calculated ~95-100 km in the western Pyrenees [*Teixell et al., 2016*], ~122-  
572 142 km [*Mouthereau et al., 2014*] in the central Pyrenees, and ~125 km (*Vergés et al., 2005*)  
573 in the eastern Pyrenees for approximately the same period (Late Cretaceous–Eocene period).  
574 This eastward increase of the shortening amount might result from a higher amount of  
575 subduction in the Provence segment, which is consistent with counter-clockwise rotation of  
576 the Sardinia block with respect to Iberia during the Pyrenean–Provence contractional period  
577 [*Advokaat et al., 2014*].

578

## 579 **6. Conclusions**

580

581 Surface structural data, seismic profiles, exploration wells, and previously published deep  
582 geophysical data together with tectonic map reconstructions have been combined here with  
583 crustal-scale to lithospheric-scale structural balancing techniques. These have thus contributed  
584 to an understanding of the dynamics of the Provence Chain and its long-term history of  
585 deformation insight into the Pyrenean and Mediterranean geodynamics.

586         The construction of two crustal-scale sections (~120 km long) across the present  
587 Provence belt indicates various structural styles that include deep-seated basement faults that

588 affect the entire crust, tectonic inversions of Paleozoic–Mesozoic basins, shallower  
589 décollements within sedimentary cover, and salt diapirism. The thrust belt is also  
590 characterized by heterogeneous shortening along the strike, accommodated by a regional  
591 accommodation zone, the Aix-Middle Durance fault system, overlying a Paleozoic basement  
592 grain.

593         Although Oligocene–Miocene rifting and Neogene Alpine compression led to  
594 additional structural complexity (including the Ligurian continental break-up and the counter-  
595 clockwise rotation of the Sardinia–Corsica block), this deformation is small (1.5 km of  
596 horizontal tectonic movement) across the present Provence belt in comparison with the  
597 Pyrenean–Provence deformation (up to 46.4 km of shortening). Consequently, the major trend  
598 of the present-day tectonic framework of Provence belt results from the Late Cretaceous–  
599 Eocene compression.

600         The construction of a sequentially restored cross-section across the Provence–Sardinia  
601 orogen (~400 km long) at the scale of the lithosphere suggests strong similarities between  
602 Provence and Pyrenean geodynamics. The Provence belt shows evidence for Middle  
603 Cretaceous rifting between Eurasia and Sardinia that links the Pyrenean rift to the west and  
604 the Valais domain to the northeast. Restoration suggests a partitioned rift system with crustal  
605 hyper-extension. The total crustal extension achieved in this zone is estimated at least of 40-  
606 45 km. During Late Cretaceous–Eocene inversion, the Eurasian lithosphere formed a rigid  
607 indent into the Sardinia lithosphere at the crust–mantle boundary. This shortening was  
608 accommodated by inversion of N-verging inherited crustal faults and N-directed subduction  
609 of the Sardinia mantle lithosphere under the Provence associated with ductile thickening of  
610 the Provence mantle lithosphere. The total crustal shortening in the Provence segment reaches  
611 ~155 km (35%). This value is higher than in the Pyrenees for the same period. It might result

612 from an eastward increase in the amount of subduction associated with counter-clockwise  
613 rotation of the Sardinia with respect to Iberia during the Pyrenean–Provence compression.

614 This study shows the prime control of the Variscan structural inheritance over a long  
615 period of time on the tectonic evolution of a geological system, the Provence orogen. This  
616 includes mechanical heterogeneities, such as Late Paleozoic rift structures and shear zones,  
617 reactivated during Middle Cretaceous rifting between Eurasia and Sardinia. In domains where  
618 Mesozoic rifting is well marked, inherited basement normal faults and the weak crust favored  
619 the formation of an inner thick-skinned thrust belt during Late Cretaceous–Eocene  
620 contraction. During the Oligocene, these domains were still predisposed for the localized  
621 faulting of the Ligurian basin rifting and the seafloor spreading between Provence and  
622 Sardinia.

623

#### 624 **Acknowledgments**

625 This research project was co-financed by the Commissariat à l'Énergie Atomique et aux  
626 Énergies Alternatives (CEA; CASHIMA program), the French CNRS-INSU program  
627 SYSTER, and by the PACA region. Midland Valley is acknowledged for providing academic  
628 license of “Move” for structural modeling. We thank C. Montenat, J.-M. Triat, J. Philip, M.  
629 Floquet, S. Leleu, N. Cherpeau, J. Giuliano, and A. Masrouhi for fieldwork and helpful  
630 discussions. C. Berrie provided valuable improvement of an earlier version of the manuscript.  
631 We acknowledge the Associate Editor, Nicolas Bellahsen, François Roure and an anonymous  
632 reviewer for the constructive comments which greatly helped us to improve our manuscript.  
633 All data for this paper is properly cited and referred to in the reference list and available by  
634 contacting the corresponding author ([espurt@cerege.fr](mailto:espurt@cerege.fr)).

635

636 **References**

- 637 Advokaat, E.L., D.J.J. van Hinsbergen, M. Maffione, C.G. Langereis, R.L.M. Vissers, A.  
638 Cherchi, R. Schroeder, H. Madani, and S. Columbu (2014), Eocene rotation of Sardinia, and  
639 the paleogeography of the western Mediterranean region, *Earth and Planetary Science Letters*,  
640 401, 183-195, 10.1016/j.epsl.2014.06.012.
- 641 Andreani, L., N. Loget, C. Rangin, and X.L. Pichon (2010), New structural constraints on the  
642 southern Provence thrust belt (France): evidence for a Eocene shortening event linked to the  
643 Corsica–Sardinia subduction, *Bull. Soc. Géol. Fr.*, 181, 547-563, doi:  
644 10.2113/gssgfbull.181.6.547.
- 645 Angelier, J., and J. Aubouin (1976), Contribution à l'étude géologique des bandes triasiques  
646 provençales: de Barjols (Var) au bas Verdon, *Bulletin du Bureau de Recherches Géologiques*  
647 *et Minières (deuxième série), Section I, 3*, 187-217.
- 648 Arnaud, H. (1988), Subsidence in certain domains of south-eastern France during the Ligurian  
649 Thetys opening and spreading stages, *Bull. Soc. Géol. Fr.*, 8, 4, 725-732.
- 650 Arnaud, M., B. Beaudoin, E. Colomb, and C. Monleau (1990), Le gypse triasique de la vallée  
651 de l'Huveaune (Bouches-du-Rhône) a été karstifié pendant le Crétacé supérieur. Implications  
652 tectoniques, *Géologie Alpine*, 66, 117-121.
- 653 Arthaud, F., and P. Matte (1975), Les décrochements tardi-hercyniens du sud-ouest de  
654 l'Europe. Géométrie et essai de reconstitution des conditions de la déformation,  
655 *Tectonophysics*, 25, 139-171, doi: 10.1016/0040-1951(75)90014-1.
- 656 Baby, P., G. Hérail, J.M. Lopez, O. Lopez, J. Oller, J. Pareja, T. Sempere, and D. Tufino,  
657 (1989), Structure de la zone subandine de Bolivie: influence de la géométrie des séries

- 658 sédimentaires antéorogéniques sur la propagation des chevauchements, Comptes rendus de  
659 l'Académie des Sciences, Ser. II., 309, 1717-1722.
- 660 Bache, F., J.L. Olivet, C. Gorini, D. Aslanian, C. Labails, and M. Rabineau (2010), Evolution  
661 of rifted continental margins: The case of the Gulf of Lions (Western Mediterranean Basin),  
662 Earth and Planetary Science Letters, 292, 345-356.
- 663 Bellahsen, N., F. Mouthereau, A. Boutoux, M. Bellanger, O. Lacombe, L. Jolivet, and Y.  
664 Rolland (2014), Collision kinematics in the western external Alps, Tectonics, 33, 1055-1088,  
665 doi:10.1002/2013TC003453.
- 666 Beltrando, M., G. Frasca, R. Compagnoni, and A. Vitale-Brovarone (2012), The Valaisan  
667 controversy revisited: Multi-stage folding of a Mesozoic hyper-extended margin in the Petit  
668 St. Bernard pass area (Western Alps), Tectonophysics, 579, 17-36,  
669 doi:10.1016/j.tecto.2012.02.010.
- 670 Benedicto, A., P. Labaume, M. Séguret, and M. Séranne (1996), Low-angle crustal ramp and  
671 basin geometry in the Gulf of Lion passive margin: Oligocene-Aquitainian Vistrenque graben,  
672 SE France, Tectonics, 15, 1192-1212, doi: 10.1029/96TC01097.
- 673 Bergerat, F. (1987), Stress fields in the European platform at the time of Africa-Eurasia  
674 collision, Tectonics, 6, 99-132, doi: 10.1029/TC006i002p00099.
- 675 Besson, D. (2005), Architecture du bassin rhodano-provençal miocène (Alpes, SE France),  
676 Relations entre déformation, physiographie et sédimentation dans un bassin molassique  
677 d'avant-pays, PhD thesis, Ecole des Mines de Paris, 438p.

- 678 Bestani, L., N. Espurt, J. Lamarche, M. Floquet, J. Philip, O. Bellier, and F. Hollender (2015),  
679 Structural style and evolution of the Pyrenean–Provence thrust belt, SE France, Bull. Soc.  
680 Géol. Fr., 186, 223-241.
- 681 Bestani, L. (2015), Géométrie et cinématique de l'avant-pays provençal: Modélisation par  
682 coupes équilibrées dans une zone à tectonique polyphasée, PhD thesis, Aix-Marseille  
683 Université, 250p.
- 684 Boyer, S. E., and D. Elliott (1982), The geometry of thrust systems, Am. Assoc. Pet.  
685 Geol. Bull., 66, 1196-1230.
- 686 Burg, J. P., J. P. Brun, and J. van den Driessche (1990), Le Sillon Houiller du Massif Central  
687 français: Faille de transfert pendant l'amincissement crustal de la chaîne varisque?, C. R.  
688 Acad. Sci., 311, 147-152.
- 689 Busulini, A., I. Dieni, F. Massari, D. Pejović, and J. Wiedmann (1984), Nouvelles données  
690 sur le Crétacé Supérieur de la Sardaigne Orientale, Cretaceous Research, 5, 243-258.
- 691 Butler, R.W.H. (2013), Area balancing as a test of models for the deep structure of mountain  
692 belts, with specific reference to the Alps, J. Struct. Geol., 52, 2-16.
- 693 Butler, R.W.H., E. Tavarnelli, and M. Grasso (2006), Structural inheritance in mountain belts:  
694 an Alpine-Apennine perspective, J. Struct. Geol., 28(11), 1893-1908.
- 695 Carosi, R., C. Frassi, D. Iacopini, and C. Montomoli (2005), Post collisional transpressive  
696 tectonics in northern Sardinia (Italy), J. Virtual Explorer, 19, paper 3.
- 697 Casagrande, L., J. Andrieux, and J.L. Morel (1989), Le massif de Suzette (Vaucluse):  
698 l'inversion tectonique d'un graben oligocène, Géologie de la France, 3, 3-12.

- 699 Champion, C., P. Choukroune, and G. Clauzon (2000), La déformation post-Miocène en  
700 Provence occidentale, *Geodinamica Acta*, 13, 67-85, doi: 10.1016/S0985-3111(00)00114-5.
- 701 Cherchi, A., N. Mancin, L. Montadert, M. Murru, M. Terasa Putzu, F. Schiavinotto, and V.  
702 Verrubbi (2008), Les conséquences stratigraphiques de l'extension oligo-miocène en  
703 Méditerranée occidentale à partir d'observations dans le système de grabens de Sardaigne  
704 (Italie), *Bull. Soc. Géol. Fr.*, 179, 267-287.
- 705 Chorowicz, J., and A. Mekarnia (1992), Evidence of a NW-SE striking Albo-Aptian  
706 extensional event in Provence (southeastern France), *C.R. Acad. Sci. Paris* 315, 861-866.
- 707 Choukroune, P., B. Pinet, F. Roure, and M. Cazes (1990), Major Hercynian thrust along the  
708 ECORS Pyrenees and Biscay lines, *Bull. Soc. Géol. Fr.*, 2, 313-320,  
709 doi:10.2113/gssgfbull.VI.2.313.
- 710 Clauzon, G., and C. Gouvernet (1973), Sur la présence d'une brèche syn-orogénique d'âge  
711 paléogène dans le chaînon du Petit Luberon (Vaucluse), *C.R. Acad. Sci. Paris* 277, (D),  
712 2637-2640.
- 713 Clauzon, G., J.-P. Suc, F. Gautier, A. Berger, and M.-F. Loutre (1996), Alternate  
714 interpretation of the Messinian salinity crisis: controversy resolved?, *Geology*, 24, 363-366,  
715 doi: 10.1130/0091-7613(1996)024<0363:AIOTMS>2.3.CO;2.
- 716 Clauzon, G., T.-J. Fleury, O. Bellier, S. Molliex, L. Mocochain, and J.-P. Aguilar (2011),  
717 Morphostructural evolution of the Luberon since the Miocene (SE France), *Bull. Soc. Géol.*  
718 *Fr.*, 182, 95-110.

- 719 Clerc, C., Y. Lagabriele, M. Neumaier, J.-Y. Reynaud, and M. de Saint Blanquat (2012),  
720 Exhumation of subcontinental mantle rocks: evidence from ultramafic-bearing clastic deposits  
721 nearby the Lherz peridotite body, French Pyrenees, *Bull. Soc. Géol., Fr.*, 183(5), 443-459.
- 722 Clerc, C., and Y. Lagabriele (2014), Thermal control on the modes of crustal thinning leading  
723 to mantle exhumation: Insights from the Cretaceous Pyrenean hot paleomargins, *Tectonics*,  
724 33, 1340–1359, doi:10.1002/2013TC003471.
- 725 Colletta, B., F. Roure, B. de Toni, D. Loureiro, H. Passalacqua, and Y. Gou (1997), Tectonic  
726 inheritance, crustal architecture, and contrasting structural styles in the Venezuela Andes,  
727 *Tectonics*, 16, 777-794, doi: 10.1029/97TC01659.
- 728 Corroy, G., and J. Philip (1964), Le brachyantoclinal des pics des Corbeaux, dans le massif de  
729 la Sainte-Baume (Var), *Bull. Soc. Géol., Fr.*, 7, 560-563.
- 730 Coward, M.P. (1996), Balancing sections through inverted basins. In: Buchanan, P.G., and  
731 Neuwland, D.A. (eds), *Modern Developments in Structural Interpretation, Validation and*  
732 *Modelling*, Geological Society Special Publication, 99, 51-77.
- 733 Cushing, E.M., O. Bellier, S. Nechtschein, M. Sébrier, A. Lomax, P. Volant, P. Dervin, P.  
734 Guignard, and L. Bove (2008), A multidisciplinary study of a slow-slipping fault for seismic  
735 hazard assessment: the example of the Middle Durance Fault (SE France), *Geophysical*  
736 *Journal International*, 172, 1163-1178, doi: 10.1111/j.1365-246X.2007.03683.x.
- 737 Danišik, M., J. Kuhlemann, I. Dunkl, B. Székely, and W. Frisch (2007), Burial and  
738 exhumation of Corsica (France) in the light of fission track data, *Tectonics*, 26, TC1001,  
739 doi:10.1029/2005TC001938.

- 740 Dahlstrom, C.D.A. (1969), Balanced cross-sections, *Canadian Journal of Earth Sciences*, 6(4),  
741 743-757.
- 742 Debroas, E.J. (1990), Le Flysch noir albo-cénomanién témoin de la structuration albienne à  
743 sénonienne de la Zone nord-pyrénéenne en Bigorre (Hautes-Pyrénées, France), *Bull. Soc.*  
744 *Géol. Fr.*, 8, 273-285.
- 745 de Graciansky, P.C., and M. Lemoine (1988), Early Cretaceous tectonics in the southwestern  
746 French Alps: a consequence of North Atlantic rifting during Tethyan spreading, *Bull. Soc.*  
747 *Géol. Fr.*, 5, 733-737.
- 748 Delfaud, J., N. Toutin-Morin, and R. Morin (1989), Un cône alluvial en bordure d'un bassin  
749 intramontagneux: la formation permienne du Rocher de Roquebrune (Bassin du Bas-Argens,  
750 Provence orientale), *Comptes rendus de l'Académie des sciences, Série 2, Mécanique,*  
751 *Physique, Chimie, Sciences de l'Univers, Sciences de la Terre*, 309, 1811-1817.
- 752 Demory, F., G. Conesa, J. Oudet, H. Mansouri, P. Münch, J. Borgomano, N. Thouveny, J.  
753 Lamarche, F. Gisquet, and L. Marié (2011), Magnetostratigraphy and paleoenvironments in  
754 shallow-water carbonates: the Oligocene-Miocene sediments of the northern margin of the  
755 Liguro-Provençal basin (West Marseille, southeastern France), *Bull. Soc. Géol. Fr.*, 182, 37-  
756 55.
- 757 Dèzes, P., S.M. Schmid, and P.A. Ziegler (2004), Evolution of the European Cenozoic Rift  
758 System: interaction of the Alpine and Pyrenean orogens with their foreland lithosphere,  
759 *Tectonophysics*, 389, 1-33, doi: 10.1016/j.tecto.2004.06.011.
- 760 Dubois, P. (1966), Sur la sédimentation et la tectonique du Miocène de la Provence  
761 occidentale, *Bull. Soc. Géol. Fr.*, 7, 793-801.

- 762 Duée, G., Y. Lagabriele, A. Coutelle, and A. Fortané (1984), Les lherzolites associées aux  
763 Chaînons Béarnais (Pyrénées Occidentales): mise à l'affleurement anté-dogger et  
764 resédimentation albo-cénomanienne, C. R. Acad. Sci., Ser. II, 299, 1205-1209.
- 765 Dufaure, P., J. Ferrat, A. Laumondais, and M. Mille (1969), Description sommaire d'un  
766 sondage dans la chaîne de Martigues (Bouches-du-Rhône), Bull. Soc. Géol. Fr., 5, 670-675.
- 767 Espurt, N., S. Brusset, P. Baby, W. Hermoza, R. Bolaños, D. Uyen, and J. Déramond (2008),  
768 Paleozoic structural controls on shortening transfer in the Subandean foreland thrust system,  
769 Ene and southern Ucayali basins, Peru, Tectonics, 27, TC3009, doi:10.1029/2007TC002238.
- 770 Espurt, N., J.-C. Hippolyte, M. Saillard, and O. Bellier (2012), Geometry and kinematic  
771 evolution of a long-living foreland structure inferred from field data and cross section  
772 balancing, the Sainte-Victoire System, Provence, France, Tectonics, 31, TC4021, doi:  
773 10.1029/2011TC002988.
- 774 Espurt, N., J.-C. Hippolyte, N. Kaymakci, and E. Sangu, (2014), Lithospheric structural  
775 control on inversion of the southern margin of the Black Sea Basin, Central Pontides, Turkey,  
776 Lithosphere, 6, 26-34, doi: 10.1130/L316.1.
- 777 Faulds, J.E., and J.V. Robert (1998), The role of accommodation zones and transfer zones in  
778 the regional segmentation of extended terranes, in Accommodation zones and transfer zones;  
779 the regional segmentation of the Basin and Range Province, Geological Society of America  
780 Special Paper, 323, 1-45.
- 781 Fellin, M. G., V. Picotti, and M. Zattin (2005), Neogene to Quaternary rifting and inversion in  
782 Corsica: Retreat and collision in the western Mediterranean, Tectonics, 24, TC1011,  
783 doi:10.1029/2003TC001613.

- 784 Floquet, M., J. Gari, J. Hennuy, P. Léonide, and J. Philip (2005), Sédimentations gravitaires  
785 carbonatées et silicoclastiques dans un bassin en transtension, séries d'âge céno-manien à  
786 coniacien moyen du Bassin sud-provençal, Publ. Association des Sédimentologues Français,  
787 52, 80 p.
- 788 Ford, M., and U. Stahel (1995), The geometry of a deformed carbonate slope-basin transition:  
789 The Ventoux-Lure fault zone, SE France, *Tectonics*, 14, 1393-1410.
- 790 Garibaldi, C., L. Guillou-Frottier, J.-M. Lardeaux, D. Bonte, S. Lopez, V. Bouchot, and P.  
791 Ledru (2010), Thermal anomalies and geological structures in the Provence Basin;  
792 implications for hydrothermal circulations at depth, *Bull. Soc. Géol. Fr.*, 181, 363-376.
- 793 Gattacceca, J., A. Deino, R. Rizzo, D.S. Jones, B. Henry, B. Beaudoin, and F. Vadeboin  
794 (2007), Miocene rotation of Sardinia: new paleomagnetic and geochronological constraints  
795 and geodynamic implications, *Earth and Planetary Science Letters*, 258, 359-377, doi:  
796 10.1016/j.epsl.2007.02.003
- 797 Guieu, G. (1973), L'évolution tectonique de la chaîne de la Nerthe, au Nord-Ouest de  
798 Marseille, *Compte Rendu de l'Académie des Sciences, Paris*, 276, 13-16.
- 799 Guignard, P., O. Bellier, and D. Chardon (2005), Géométrie et cinématique post-oligocène  
800 des failles d'Aix et de la moyenne Durance (Provence, France), *Comptes Rendus Académie  
801 des Sciences Geoscience*, 337, 375-384.
- 802 Guillot, S., and R.-P. Menot (2009), Paleozoic evolution of the External Crystalline Massifs  
803 of the Western Alps, *C. R. Geoscience*, 341, 253-265.
- 804 Guyonnet-Benaize, C., J. Lamarche, J.-P. Masse, M. Villeneuve, and S. Viseur (2010), 3D  
805 structural modelling of small-deformations in poly phase faults pattern, Application to the

- 806 Mid-Cretaceous Durance uplift, Provence (SE France), *J. Geodyn.*, 50, 81-93,  
807 doi:10.1016/j.jog.2010.03.003.
- 808 Guyonnet-Benaize, C. (2011), Modélisation 3D multi-échelle des structures géologiques de la  
809 région de la faille de la moyenne Durance (SE France). Thèse Sci., Aix-Marseille Université,  
810 Centre Saint-Charles, Marseille, 187 p.
- 811 Guyonnet-Benaize, C., J., Lamarche, F. Hollender, S. Viseur, P. Münch, and J. Borgomano  
812 (2015), Three-dimensional structural modeling of an active fault zone based on complex  
813 outcrop and subsurface data: the Middle Durance Fault Zone inherited from polyphase Meso-  
814 Cenozoic tectonics (southeastern France), *Tectonics*, 34, doi: 10.1002/2014TC003749.
- 815 Handy, M. R., S. M. Schmid, R. Bousquet, E. Kissling, and D. Bernoulli (2010), Reconciling  
816 plate-tectonic reconstructions of Alpine Tethys with the geological–geophysical record of  
817 spreading and subduction in the Alps, *Earth Sci. Rev.*, 102(3-4), 121-158,  
818 doi:10.1016/j.earscirev.2010.06.002.
- 819 Hennuy, J. (2003), Sédimentation carbonate et silicoclastique sous contrôle tectonique, le  
820 bassin sud-provençal et sa plate-forme carbonatée du Turonien au Coniacien moyen.  
821 Evolution séquentielle, diagénétique, paléogéographique. Thèse Sci., Aix-Marseille  
822 Université, Centre Saint-Charles, Marseille, 252 p.
- 823 Hippolyte, J.-C., J. Angelier, F. Bergerat, D. Nury, and G. Guieu (1993), Tectonic-  
824 stratigraphic record of paleostress time changes in the Oligocene basins of the Provence,  
825 southern France, *Tectonophysics*, 226, 15-35, doi: 10.1016/0040-1951(93)90108-V.
- 826 Homberg, C., Y. Schnyder, and M. Benzaggagh (2013), Late Jurassic-Early Cretaceous  
827 faulting in the Southeastern French basin: Does it reflect a tectonic reorganization?, *Bull. Soc.*  
828 *Geol. Fr.*, 184, 501–514.

- 829 Jakni, B. (2000), Thermochronologie par traces de fission des marges conjuguées du bassin  
830 liguro-provençal: la Corse et le massif des Maures-Tanneron. Thesis Univ. de Grenoble I, 344  
831 p.
- 832 Jammes, S., G. Manatschal, L. Lavier, and E. Masini (2009), Tectonosedimentary evolution  
833 related to extreme crustal thinning ahead of a propagating ocean: Example of the western  
834 Pyrenees, *Tectonics*, 28, TC4012, doi:10.1029/2008TC002406.
- 835 Jannin, S. (2011), Rôle de la tectonique salifère dans la structuration du bassin du Sud-Est (SE  
836 de la France): définition d'un modèle de tectonique salifère d'après l'étude du secteur de  
837 Draguignan et comparaison de ce modèle aux structures halocinétiques rencontrées sur  
838 l'ensemble du bassin. Mémoire d'Ingénieur Géologue, Institut Polytechnique Lasalle  
839 Beauvais n° 476, 97 p., 50 fig., 4 annexes.
- 840 Jiménez-Munt, I., R. Sabadini, A. Gardi, and G. Blanco (2003), Active deformation in the  
841 Mediterranean from Gibraltar to Anatolia inferred from numerical modelling and geodetic and  
842 seismological data, *J. Geophys. Res.*, 108(B1), doi:10.1029/2001JB001544
- 843 Jourdon, A., Y. Rolland, C. Petit, and N. Bellahsen (2014), Style of Alpine tectonic  
844 deformation in the Castellane fold-and-thrust belt (SW Alps, France): insights from balanced  
845 cross-sections, *Tectonophysics*, 633, 143-155, doi: 10.1016/j.tecto.2014.06.022.
- 846 Kley, J., and C.R. Monaldi (2002), Tectonic inversion in the Santa Barbara System of the  
847 central Andean foreland thrust belt, northwestern Argentina, *Tectonics*, 21, 1061, doi:  
848 10.1029/2002TC902003.
- 849 Lacombe, O., J. Angelier, and P. Laurent (1992), Determining paleostress orientations from  
850 faults and calcite twins: a case study near the Sainte-Victoire Range (southern France),  
851 *Tectonophysics*, 201, 141-156, doi: 10.1016/0040-1951(92)90180-E.

- 852 Lacombe, O., and F. Mouthereau (2002), Basement-involved shortening and deep detachment  
853 tectonics in forelands of orogens: insights from recent collision belts (Taiwan, Western Alps,  
854 Pyrenees), *Tectonics*, 21, 1030, doi: 10.1029/2001TC901018.
- 855 Lacombe, O., and L. Jolivet (2005), Structural and kinematic relationships between Corsica  
856 and the Pyrenees-Provence domain at the time of the Pyrenean orogeny, *Tectonics*, 24,  
857 TC1003, doi: 200510.1029/2004TC001673.
- 858 Lagabrielle, Y., P. Labaume, and M. de Saint Blanquat (2010), Mantle exhumation, crustal  
859 denudation, and gravity tectonics during Cretaceous rifting in the Pyrenean realm (SW  
860 Europe): insights from the geological setting of the Iherzolite bodies, *Tectonics*, 29, TC4012,  
861 doi: 10.1029/2009TC002588.
- 862 Le Pichon, X., C. Rangin, Y. Hamon, N. Loget, J.Y. Lin, L. Andreani, and N. Flotte (2010),  
863 Geodynamics of the France Southeast Basin, *Bull. Soc. Géol. Fr.*, 181, 477-501, doi:  
864 10.2113/gssgfbull.181.6.477.
- 865 Leleu, S., J.-F. Ghienne, and G. Manatschal (2009), Alluvial fan development and morpho-  
866 tectonic evolution in response to contractional fault reactivation (Late Cretaceous–  
867 Palaeocene), Provence, France, *Basin Research*, 21, 2, 157-187.
- 868 Léonide, P., J. Borgomano, J.-P. Masse, and S. Doublet (2012), Relation between  
869 stratigraphic architecture and multi-scale heterogeneities in carbonate platforms: the  
870 Barremian–lower Aptian of the Monts de Vaucluse, SE France, *Sedimentary Geology*, 265-  
871 266, 87-109, doi: 10.1016/j.sedgeo.2012.03.019.
- 872 Lucazeau, F., and D., Mailhe (1986), Heat flow, heat production and fission track data from  
873 the Hercynian basement around the Provençal Basin (Western Mediterranean),  
874 *Tectonophysics*, 128, 335-356, doi:10.1016/0040-1951(86)90300-8.

- 875 Malusà, M.G., M. Danišik, and J. Kuhlemann (2016), Tracking the Adriatic-slab travel  
876 beneath the Tethyan margin of Corsica–Sardinia by low-temperature thermochronometry,  
877 *Gondwana Research*, 31, 135-149, doi.org/10.1016/j.gr.2014.12.011
- 878 Marni, P., G. Mongelli, G. Oggiano, E. Dinelli (2007), Geological, geochemical and  
879 mineralogical features of some bauxite deposits from Nurra (western Sardinia, Italy): insights  
880 on conditions of formation and parental affinity, *International Journal of Earth Sciences*, 96,  
881 887-902.
- 882 Mascle, A., and R. Vially (1999), The petroleum systems of the Southeast Basin and Gulf of  
883 Lion (France). In: Durand, B., Jolivet, L., Horvath, F. and Séranne, M. (eds), *The*  
884 *Mediterranean Basins: Tertiary Extension within the Alpine Orogen*, Geological Society,  
885 London, Special Publications, 156, 121-140.
- 886 Masse, J.-P., and J. Philip (1976), Paléogéographie et tectonique du Crétacé moyen en  
887 Provence, *Revue de Géographie Physique et de Géologie Dynamique*, 2, 49-66.
- 888 Mattauer M., and F. Proust (1967), L'évolution structurale de la partie est du domaine  
889 pyrénéo-provençal au Crétacé et au Paléogène. Biogéographie du Crétacé–Éocène de la  
890 France méridionale, in : *Travaux du Laboratoire Géochimie-Biosphère*, 9-20.
- 891 Matte, P. (2001), The Variscan collage and orogeny ( $480 \pm 290$  Ma) and the tectonic definition  
892 of the Armorica microplate: a review, *Terra Nova*, 13, 122-128.
- 893 Ménard, G. (1980), Profondeur du socle antétriasique dans le Sud-Est de la France, *Comptes*  
894 *rendus de l'Académie des Sciences Paris*, 290, 299-302.

- 895 Molliex, S., O. Bellier, M. Terrier, J. Lamarche, G. Martelet, and N. Espurt (2011), Tectonic  
896 and sedimentary inheritance on the structural framework of Provence (SE France): importance  
897 of the Salon-Cavaillon Fault, *Tectonophysics*, 501, 1-16.
- 898 Montenat, C., P. Ott d'Estevou, M. Saillard (1986), Sur la tectonique anté-cénomaniennne du  
899 fossé de Sault-de-Vaucluse (chaînes subalpines méridionales), *Comptes rendus de l'Académie*  
900 *des Sciences Paris*, 303, 609-612.
- 901 Montenat, C., M.-C. Janin, and P. Barrier (2004), L'accident du Toulourenc : une limite  
902 tectonique entre la plate-forme provençale et le Bassin vocontien à l'Aptien–Albien (SE  
903 France), *C. R. Geoscience*, 336, 1301-1310.
- 904 Montenat, C., P. Barrier, and C. Hibschi (2005), Enregistrement des événements pyrénéo-  
905 provençaux dans les chaînes subalpines méridionales (Baronnies, France), *Géologie de la*  
906 *France*, 23-73.
- 907 Morillon, A. C. (1997), Etude thermo-chronométrique appliquée aux exhumations en contexte  
908 orogénique: Le Massif des Maures (France), et les Cordillères Bétiques (Espagne), Ph.D.  
909 thesis, 303 pp., Univ. De Nice, Nice, France.
- 910 Mouthereau, F., P.-Y. Filleaudeau, A. Vacherat, R. Pik, O. Lacombe, M.G. Fellin, S.  
911 Castellort, F. Christophoul, and E. Masini (2014), Placing limits to shortening evolution in  
912 the Pyrenees: role of margin architecture and implications for the Iberia/ Europe convergence,  
913 *Tectonics*, 33, 2283-2314, doi:10.1002/2014TC003663.
- 914 Muñoz, J.A.E. (1992), Evolution of a continental collision belt: ECORS-Pyrenees crustal  
915 balanced cross-section, in *Thrust Tectonics*, edited by K. McClay, 235-246, Chapman and  
916 Hall, London.

- 917 Onézime, J., M. Faure, and G. Crévola (1999), Étude pétro-structurale du complexe granitique  
918 Rouet-Plan-de-la-Tour (massifs des Maures et du Tanneron occidental, Var), Comptes  
919 Rendus de l'Académie des Sciences, Series IIA, Earth and Planetary Science, 328, 773-779,  
920 doi: 10.1016/S1251-8050(99)80170-0.
- 921 Oudet, J., P. Munch, J. Borgomano, F. Quillevère, M.C. Melinte-Dobrinescu, F. Demory, S.  
922 Viseur, and J.-J. Cornée (2010), Land and sea study of the northeastern Golfe du Lion rifted  
923 margin; the Oligocene-Miocene of southern Provence (Nerthe area, SE France), Bull. Soc.  
924 Géol. Fr., 181, 591-607.
- 925 Philip, J. (1970), Les formations calcaires à rudistes du Crétacé supérieur provençal et  
926 rhodanien. Thèse Sci., Université de Provence, Marseille, 438 p.
- 927 Philip, J., J. Allemann (1982), Comparaison entre les plates-formes du Crétacé Supérieur de  
928 Provence and Sardaigne, Cretaceous Research, 3, 35-45.
- 929 Philip, J., J.-P., Masse, L. Machhour (1987), L'évolution paléogéographique et structurale du  
930 front de chevauchement nord-toulonnais (Basse-Provence occidentale, France), Bull. Soc.  
931 Géol. Fr., 8, III, 541-550.
- 932 Rangin, C., X. Le Pichon, Y. Hamon, N. Loget, A. Crespy (2010), Gravity tectonics in the SE  
933 Basin (Provence, France) imaged from seismic reflection data, Bull. Soc. Géol. Fr., 181, 503-  
934 530.
- 935 Rolland, Y., M. Corsini, and A. Demoux (2009), Metamorphic and structural evolution of the  
936 Maures-Tanneron massif (SE Variscan chain): evidence of doming along a transpressional  
937 margin, Bull. Soc. Géol. Fr., 180, 217-230, doi: 10.2113/gssgfbull.180.3.217.

- 938 Rollet, N., J. Déverchère, M.-O. Beslier, P. Guennoc, J.-P. Réhault, M. Sosson, and C.  
939 Truffert (2002), Back-arc extension, tectonic inheritance, and volcanism in the Ligurian Sea,  
940 *Western Mediterranean*, *Tectonics*, 21, 10.1029/2001TC900027.
- 941 Rosenbaum, G., G. S. Lister, and C. Duboz (2002), Relative motions of Africa, Iberia and  
942 Europe during Alpine orogeny, *Tectonophysics*, 359(1–2), 117–129, doi:10.1016/S0040-  
943 1951(02)00442-0.
- 944 Rossi, P., G. Oggiano, and A. Cocherie (2009), A restored section of the “southern Variscan  
945 realm” across the Corsica-Sardinia microcontinent, *Comptes Rendus Geoscience*, 341, 224-  
946 238.
- 947 Roure, F., P. Casero, and B. Addoum (2012), Alpine inversion of the North African margin  
948 and delamination of its continental lithosphere, *Tectonics*, 31, TC3006,  
949 doi:10.1029/2011TC002989
- 950 Roure, F., P. Choukroune, X. Beràstegui, J. A. Muñoz, A. Villien, P. Matheron, M. Bareyt,  
951 M. Séguret, P. Camara, and J. Déramond (1989), ECORS deep seismic data and balanced  
952 cross sections: Geometric constraints on the evolution of the Pyrenees, *Tectonics*, 8(1), 41-50,  
953 doi:10.1029/TC008i001p00041.
- 954 Roure, F., J.-P. Brun, B. Colletta, and J. Van Den Driessche (1992), Geometry and kinematics  
955 of extensional structures in the alpine foreland basin of southeastern France, *Journal of*  
956 *Structural Geology*, 14, 503-519, doi: 10.1016/0191-8141(92)90153-N.
- 957 Roure, F., and B. Colletta (1996), Cenozoic inversion structures in the foreland of the  
958 Pyrenees and Alps, in *Peri-Tethys Memoir 2: Structure and Prospects of Alpine Basins and*  
959 *Forelands*, *Mem. du Mus. Natl. Hist. Nat.* 170, edited by P. A. Ziegler, 173-209, *Mus. Natl.*  
960 *Hist. Nat.*, Paris.

- 961 Schreiber, D., G. Giannerini, and J. M. Lardeaux (2011), The Southeast France basin during  
962 Late Cretaceous times: the spatiotemporal link between Pyrenean collision and Alpine  
963 subduction, *Geodinamica Acta*, 24, 21-35.
- 964 Séguret, M. (1972), Etude tectonique des nappes et series décollées de la partie centrale du  
965 versant sud des Pyrénées, Pub. USTELA, Montpellier, Série Géol. Struct. n° 2.
- 966 Séranne, M., A. Benedicto, P. Labaume, C. Truffert, and G. Pascal (1995), Structural style  
967 and evolution of the Gulf of Lion Oligo-Miocene rifting: role of the Pyrenean orogeny,  
968 *Marine and Petroleum Geology*, 12, 809-820, doi: 10.1016/0264-8172(95)98849-Z.
- 969 Shaw, J., C. Connors, and J. Suppe (2005), Seismic interpretation of contractional fault-  
970 related folds, *AAPG Seismic Atlas, Stud. Geol.* 53, 1-156, American Association of  
971 Petroleum Geologists, Tulsa, Okla.
- 972 Specht, M. (1989), Tectonique de chevauchement le long du profil ECORS-Pyrénées: un  
973 modèle d'évolution de prisme d'accrétion continental, PhD thesis, Université de Bretagne  
974 Occidentale de Brest (Sciences), 99, 353 pp.
- 975 Stampfli, G. M., J. Mosar, D. Marquer, R. Marchant, T. Baudin, and G. Borel (1998),  
976 Subduction and obduction processes in the Swiss Alps, *Tectonophysics*, 296, 159-204.
- 977 Suppe, J. (1983), Geometry and kinematics of fault-bend folding, *American Journal of*  
978 *Science*, 283, 684-721.
- 979 Suppe, J., and D. A. Medwedeff (1990), Geometry and kinematics of fault-propagation  
980 folding, *Eclogae Geologicae Helvetiae*, 83(3), 409-454.

- 981 Teixell, A., P. Labaume, and Y. Lagabrielle (2016), The crustal evolution of the west-central  
982 Pyrenees revisited: Inferences from a new kinematic scenario, *Comptes Rendus Geoscience*,  
983 in press, doi:10.1016/j.crte.2015.10.010
- 984 Tempier, C. (1987), Modèle nouveau de mise en place des structures provençales, *Bull. Soc.*  
985 *Géol. Fr.*, 8, 533-540.
- 986 Terrier, M., O. Serrano, and F. Hanot (2008), Reassessment of the structural framework of  
987 western Provence (France): consequence on the regional seismotectonic model, *Geodinamica*  
988 *Acta*, 21, 231-238, doi: 10.3166/ga.21.231-238.
- 989 Tesauro, M., M.K. Kaban, and A.P.L. Cloetingh (2009), How rigid is Europe's lithosphere?,  
990 *Geophys. Res. Lett.*, 36, L16303, doi:10.1029/2009GL039229.
- 991 Tesauro, M., M.K. Kaban, and A.P.L. Cloetingh (2008), A new reference model for the  
992 European crust. S. A. P. L., *EuCRUST-07*, *Geophys. Res. Lett.*, 35, L05313, 1-5.
- 993 Toutin-Morin, N., D. Bonijoly, C. Brocard, and M. Dubard (1993), Enregistrement  
994 sédimentaire de l'évolution post-hercynienne en bordure des Maures et du Tanneron, du  
995 Carbonifère supérieur à l'actuel, *Géologie de la France*, 2, 3-22.
- 996 Vacherat, A., F. Mouthereau, R. Pik, M. Bernet, C. Gautheron, E. Masini, L. Le Pourhiet, B.  
997 Tibari, and A. Lahfid (2014), Thermal imprint of rift-related processes in orogens as recorded  
998 in the Pyrenees, *Earth Planet. Sci. Lett.*, 408(0), 296–306.
- 999 Vergés, J., and J. García-Senz (2001), Mesozoic evolution and Cainozoic inversion of the  
1000 Pyrenean Rift, in P.A. Ziegler, W. Cavazza, A.H.F. Robertson and S. Crasquin-Soleau (eds),  
1001 *Peri-Tethys Memoir 6: Peri-Tethyan Rift/Wrench Basins and Passive Margins. Mém. Mus.*  
1002 *natn. Hist. nat.*, 186, 187-212.

- 1003 Vially, R., and P. Trémoilières (1996), Geodynamics of the Gulf of Lions: implications for  
1004 petroleum exploration, in *Peri-Téthys Mem.*, vol. 2, *Mém. Mus. Nat. Hist. Nat.*, 170,  
1005 Structure and Prospects of Alpine Basins and Forelands, edited by P. A. Ziegler and F.  
1006 Horvath, 129-158, Ed. du Mus., Paris.
- 1007 Villegger, M., and J. Andrieux (1987), Phases tectoniques post-éocènes et structuration  
1008 polyphasée du panneau de couverture nord provençal (Alpes externes méridionales), *Bull.*  
1009 *Soc. Géol. Fr.*, 8, t. III, n° 1, 147-156.
- 1010 Wallace, W.K. (2008), Yakataga Fold-and-Thrust Belt: Structural Geometry and Tectonic  
1011 Implications of a Small Continental Collision Zone, in *Active Tectonics and Seismic Potential*  
1012 of Alaska (eds Freymueller, J.T., Haeussler, P.J., Wesson, R.L., and Ekström, G.), American  
1013 Geophysical Union, Washington, D.C., doi: 10.1029/179GM13.
- 1014 Zarki-Jakni, B., P. van der Beek, G. Poupeau, M. Sosson, E. Labrin, P. Rossi, and J.  
1015 Ferrandini (2004), Cenozoic denudation of Corsica in response to Ligurian and Tyrrhenian  
1016 extension: Results from apatite fission track thermochronology, *Tectonics*, 23, TC1003,  
1017 doi:10.1029/2003TC001535.
- 1018 Ziegler, P.A., J.-D. van Wees, and S. Cloetingh (1998), Mechanical controls on collision-  
1019 related compressional intraplate deformation, *Tectonophysics*, 300, 103-129,  
1020 doi:10.1016/S0040-1951(98)00236-4.
- 1021

1022 **Figure 1.** Geological and structural settings of the Provence basin (modified from *Bestani et*  
1023 *al.*, 2015). Cross-sections (T1 and T2) and wells are shown. Synthetic stratigraphic and  
1024 lithotectonic sedimentary columns of the western thin-skinned Provence domain and eastern  
1025 thick-skinned Provence domain are shown. Major unconformities are enhanced by a wavy  
1026 line. Major décollement levels are shown. Co: Corsica. Sa: Sardinia. LC Cg: La Ciotat  
1027 conglomerates. Bx: Bauxite

1028

1029 **Figure 2.** Tectonic map reconstructions of the Pyrenean–Provence orogenic system and  
1030 western Mediterranean Sea from Paleozoic to present day (based on *Choukroune et al.* [1990],  
1031 *Matte* [2001], *Dèzes et al.* [2004], *Lacombe and Jolivet* [2005], *Guillot and Menot* [2009],  
1032 *Bache et al.* [2010], *Molli and Malavieille* [2011], and *Advokaat et al.* [2014]). Location of  
1033 cross-section T1' (Fig. 9) is shown. CF: Cévennes fault. NF: Nîmes fault. AF: Aix-en-  
1034 Provence fault. MDF: Middle Durance fault. TF: Toulouse fault. MTM: Maures Tanneron-  
1035 Esterel massifs. TS: Tyrrhenian Sea.

1036

1037 **Figure 3.** Balanced and restored cross-section T1. (a) Present day. (b) Late Eocene state at the  
1038 end of the Pyrenean orogeny. (c) Santonian before the Pyrenean–Provence compression. For  
1039 location, see Figure 1. MDFZ: Middle Durance fault zone.

1040

1041 **Figure 4.** Balanced and restored cross-section T2. (a) Present day. (b) Late Eocene–Late  
1042 Eocene state at the end of the Pyrenean orogeny. (c) Santonian before the Pyrenean–Provence  
1043 compression. For location, see Figure 1.

1044

1045 **Figure 5.** Examples of restoration of the Pyrenean–Provence thrusts (thick red lines). (a) The  
1046 Sainte–Baume (1) and Aurélien (2) thrusts were deformed by a set of high-dipping normal

1047 faults, which included migration of Triassic salt (Huveaune basin). (b) Formation of the  
1048 Oligocene St. Julien basin above the Nerthe thrust (3). (c) Formation of the Oligocene-  
1049 Miocene Malaucène basin above the Ventoux thrust (4). For location, see Figures 3 and 4. Li:  
1050 Initial length. Lf: Final length.

1051

1052 **Figure 6.** Interpretation of seismic profile 82SE4D across the Istres syncline close to section  
1053 T2. For location, see Figures 1 and 4a (cross-section T2).

1054

1055 **Figure 7.** Interpretations of seismic profile 71D10 (a) and VL85J (b) across the eastern  
1056 Luberon anticline and Middle Durance fault zone. For location, see Figures 1 and 3a (cross-  
1057 section T1).

1058

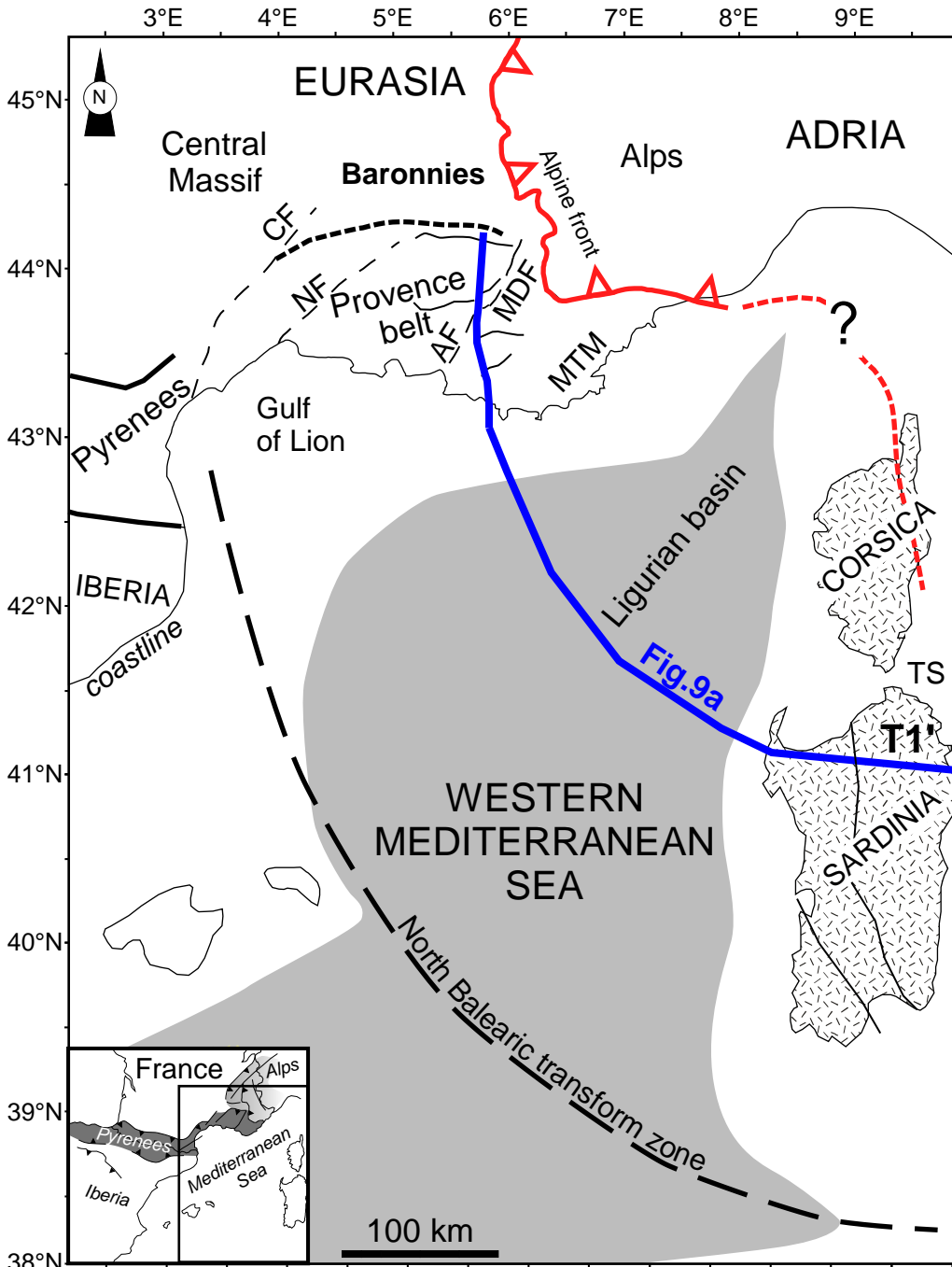
1059 **Figure 8.** East-looking panoramic view of the Ventoux thrust and Miocene Malaucène basin.  
1060 The Ventoux thrust is cut by an Oligocene normal fault sealed by Miocene foresets  
1061 [Casagrande *et al.*, 1989]. This observation provides evidence for major pre-structuration of  
1062 Ventoux thrust during the Pyrenean–Provence compression. Bedding traces are enhanced by  
1063 black lines. UTM31 view location: 667727; 4893779. For location, see also Figures 1, 4a  
1064 (cross-section T2) and 5c.

1065

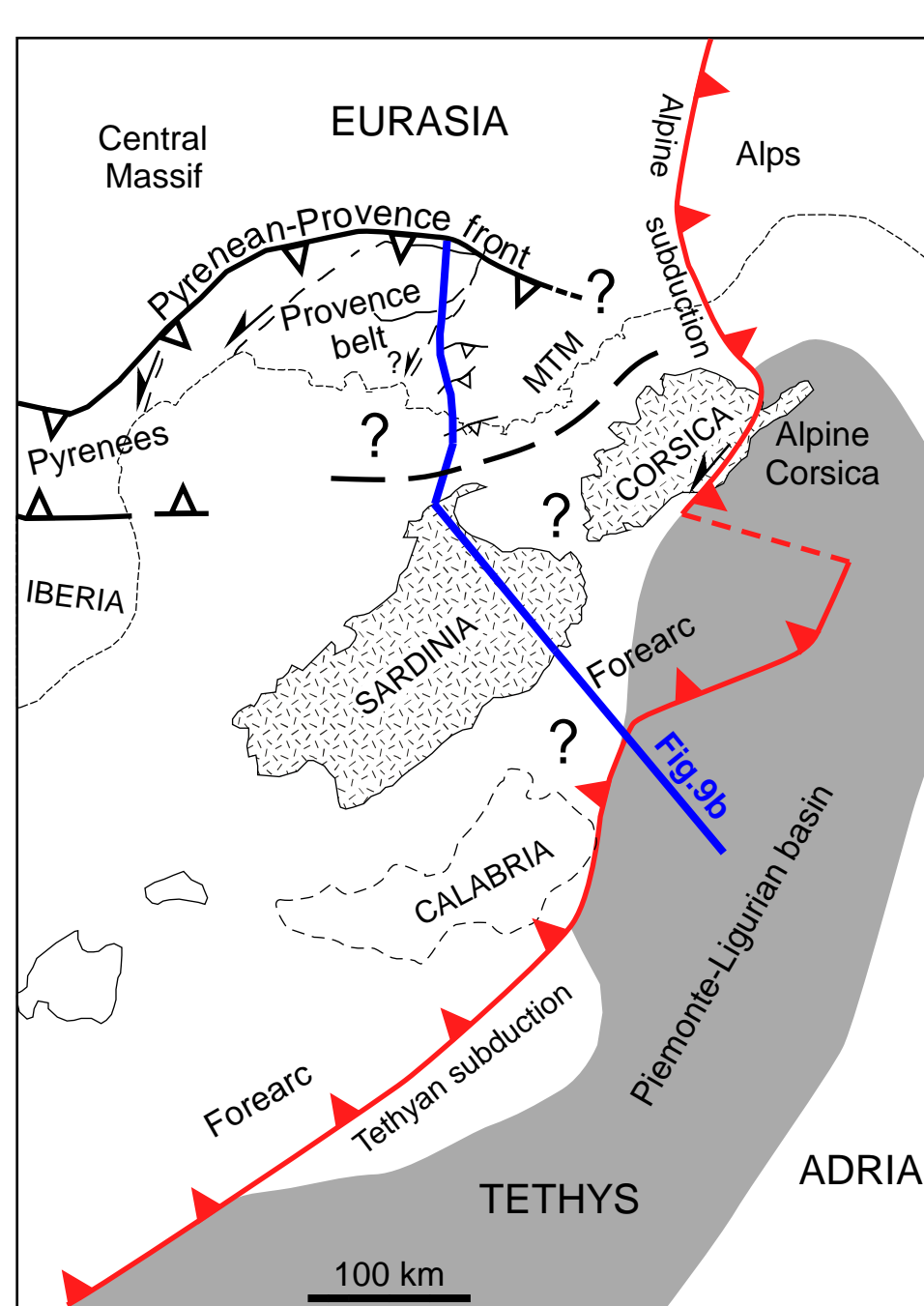
1066 **Figure 9.** Lithospheric-scale balanced and restored cross-section T1' across the entire  
1067 Pyrenean–Provence orogenic system along cross-section T1 and Sardinia. Crustal and  
1068 lithosphere thickness determined by deep geophysical data from *Jiménez-Munt et al.* [2003]  
1069 (black point), *Tesauro et al.* [2008] and *Garibaldi et al.* [2010] (red points). See details in text  
1070 and legend in Figure 3. For location, see Figure 2. MDFZ: Middle Durance fault zone. SVM:  
1071 Sainte–Victoire Mountain. AM: Aurélien Mount. SB: Sainte–Baume. B: Bandol. CS: Cap

- 1072 Sicié. VB: Vocontian basin. DU: Durance uplift. BB: Beausset basin. Ext.: Extension. Short.:
- 1073 Shortening.

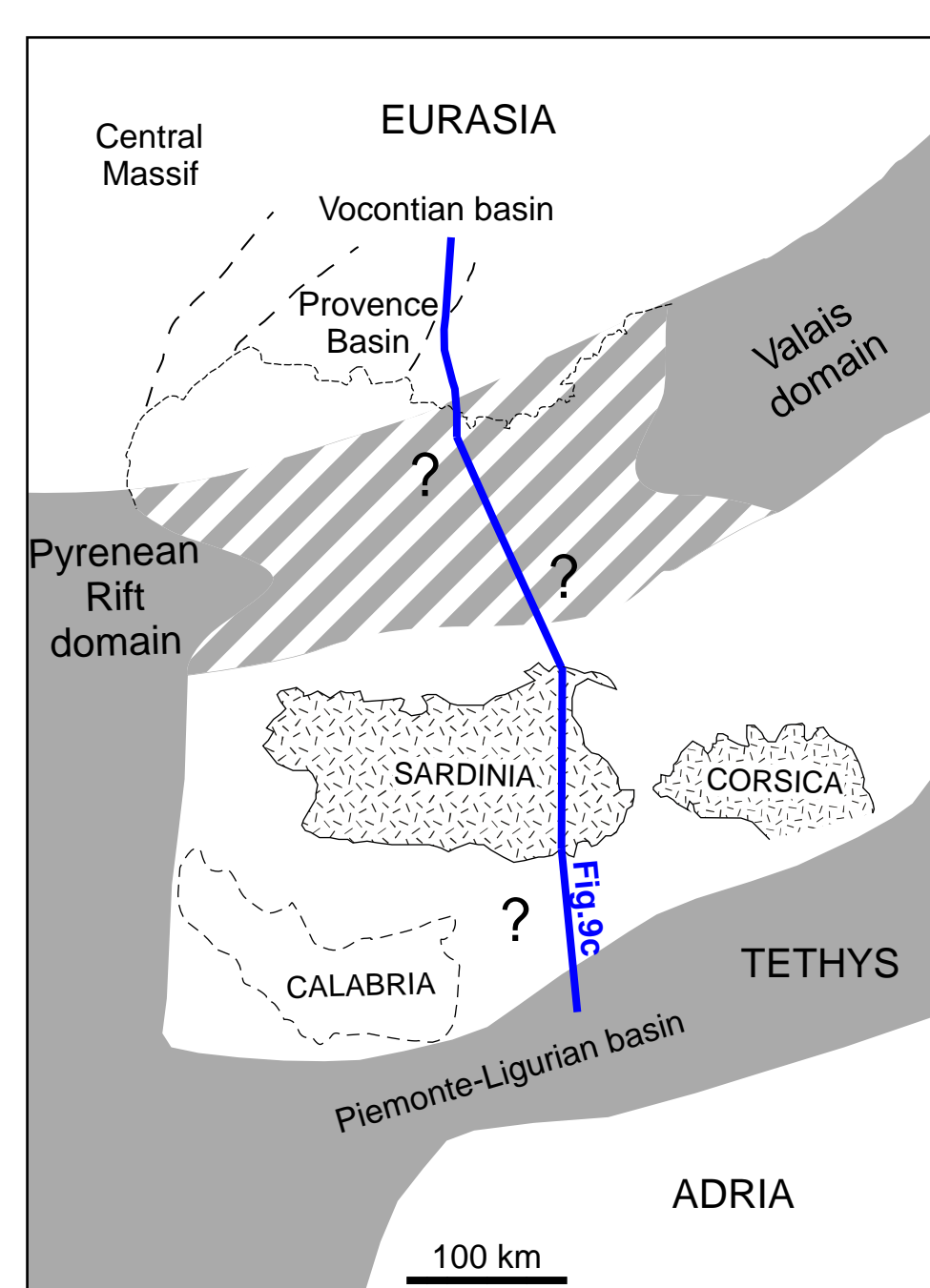




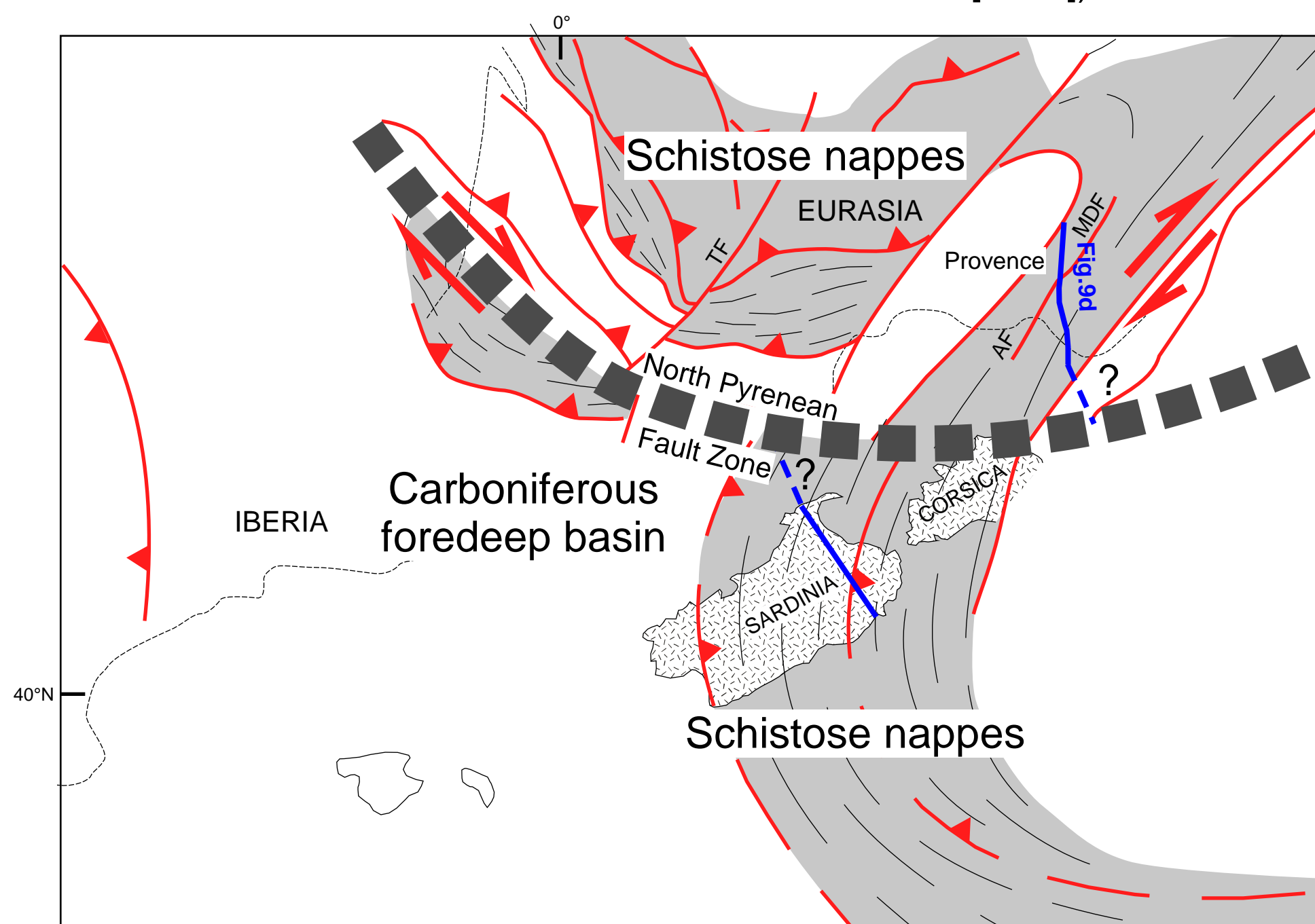
(a) Present day map (after *Dèzes et al. [2004]*, *Lacombe and Jolivet [2005]* and *Bache et al. [2010]*)



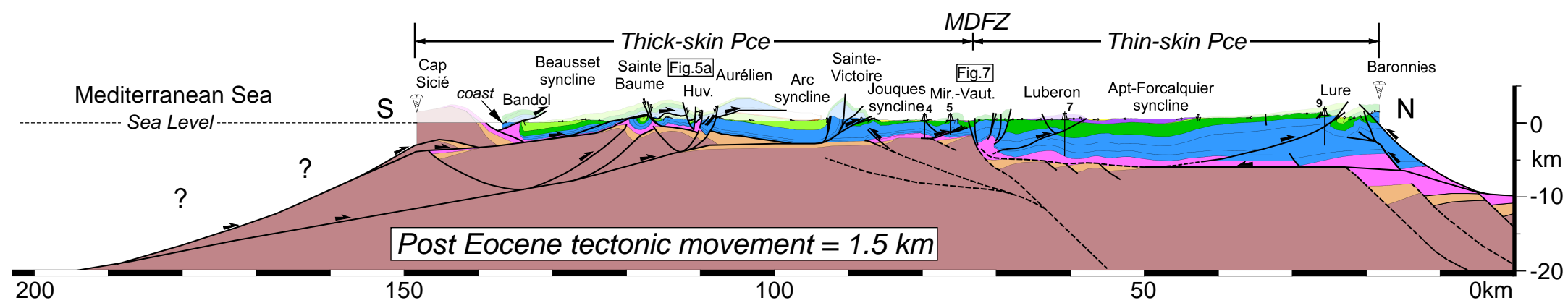
(b) Late Eocene map restoration (after *Lacombe and Jolivet [2005]*, *Molli and Malavieille [2011]* and *Advokaat et al. [2014]*)



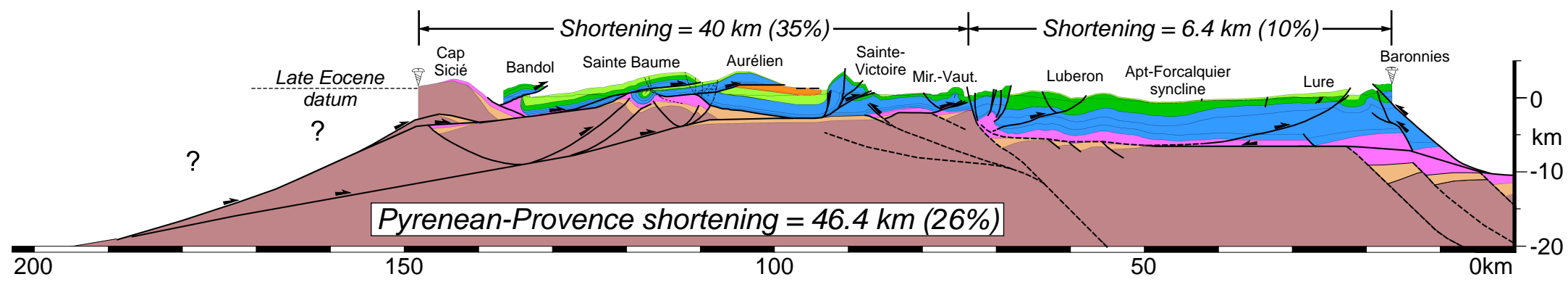
(c) Middle Cretaceous map restoration (after *Advokaat et al. [2014]*)



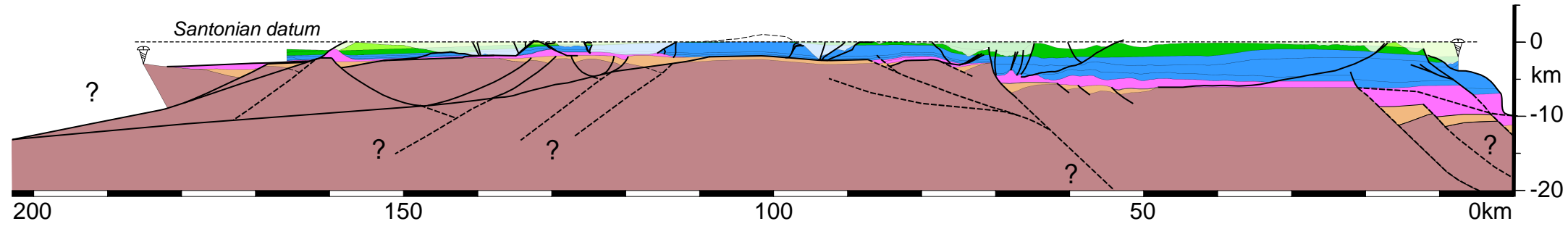
(d) Late Paleozoic map restoration (after *Choukroune et al. [1990]*, *Matte [2001]* and *Guillot and Menot [2009]*)



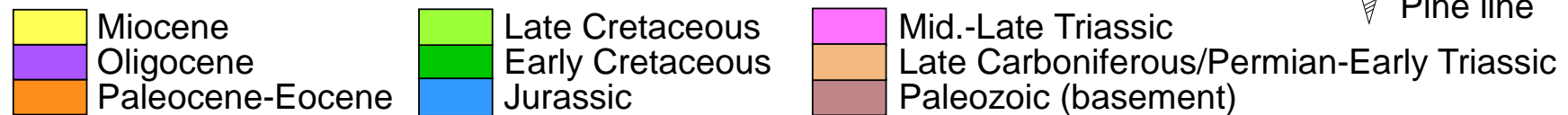
(a) Present-day

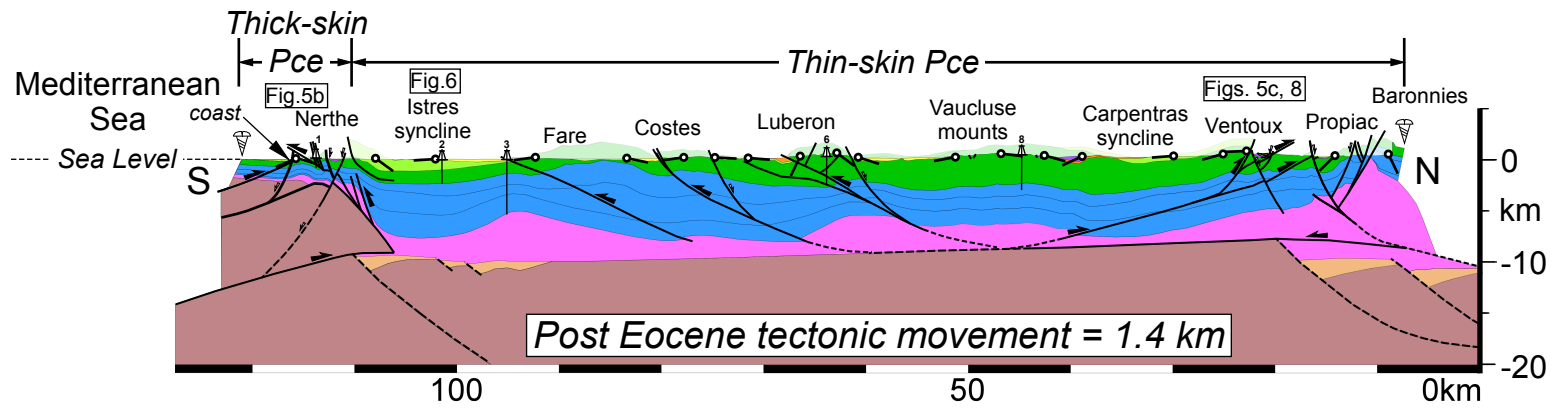


(b) Late Eocene

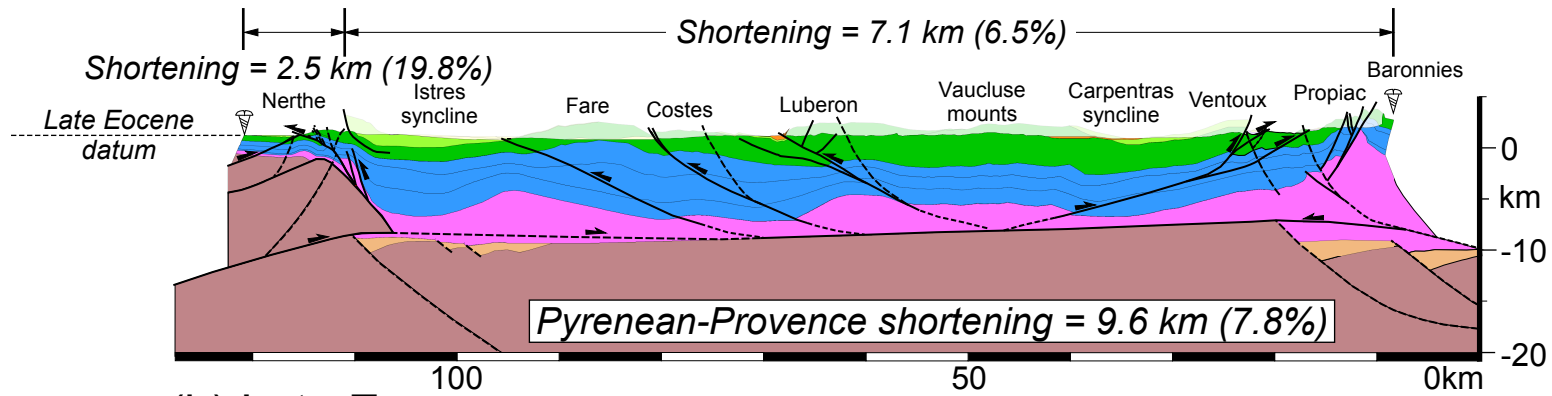


(c) Santonian

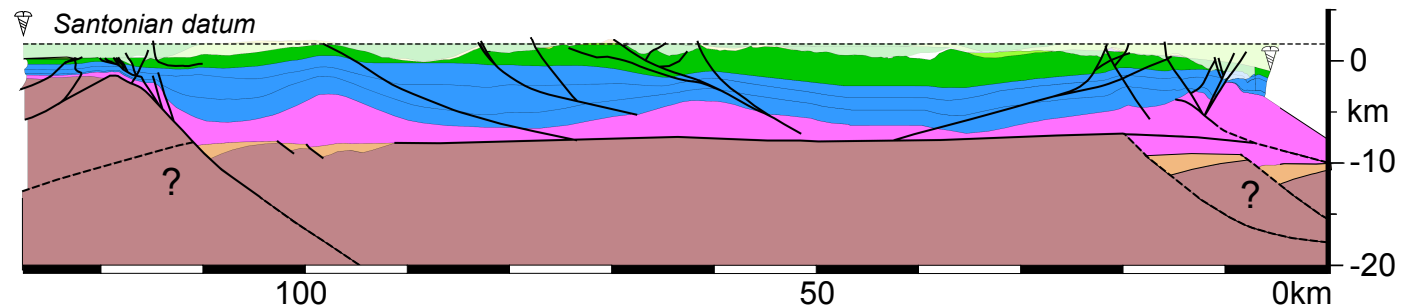




(a) Present-day



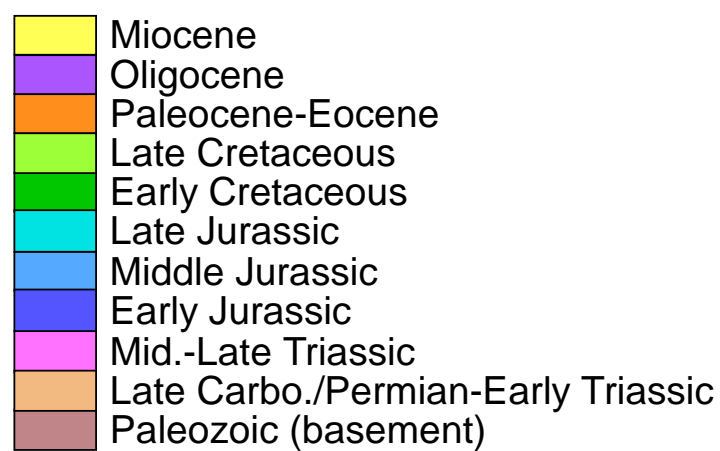
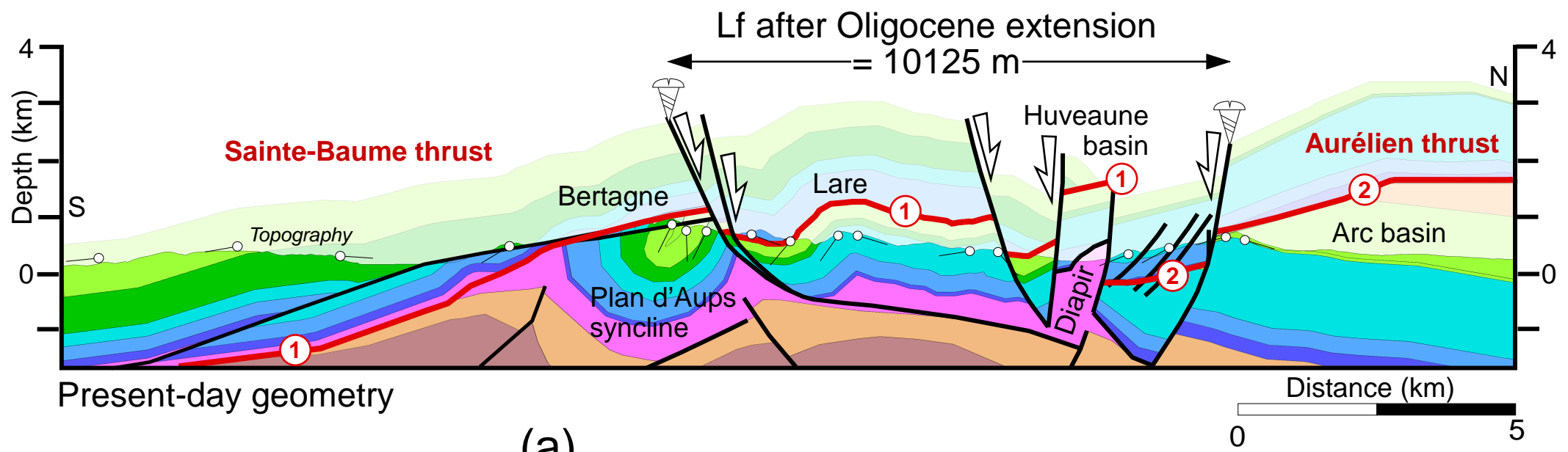
(b) Late Eocene



(c) Santonian

🌲 Pine line





🌲 Pine line

